Investigating the energy demand and supply of a residential neighborhood in Malmö

Tianqi Wang

Master thesis in Energy-efficient and Environmental Buildings
Faculty of Engineering | Lund University

Lund University

Lund University, with eight faculties and a number of research centres and specialized institutes, is the largest establishment for research and higher education in Scandinavia. The main part of the University is situated in the small city of Lund which has about 112 000 inhabitants. A number of departments for research and education are, however, located in Malmö. Lund University was founded in 1666 and has today a total staff of 6 000 employees and 47 000 students attending 280 degree programmes and 2 300 subject courses offered by 63 departments.

Master Programme in Energy-efficient and Environmental Building Design

This international programme provides knowledge, skills and competencies within the area of energy-efficient and environmental building design in cold climates. The goal is to train highly skilled professionals, who will significantly contribute to and influence the design, building or renovation of energy-efficient buildings, taking into consideration the architecture and environment, the inhabitants' behaviour and needs, their health and comfort as well as the overall economy.

The degree project is the final part of the master programme leading to a Master of Science (120 credits) in Energy-efficient and Environmental Buildings.

Examiner: PETTER WALLENTÉN (Building Physics)

Supervisor: VAHID NIK (Building Physics)

Keywords: Building energy performance, Solar energy, Micro wind turbine, Residential buildings.

Thesis: EEBD - 01 / 18

Abstract

Facing the climate change and the energy crisis, the governments are taking steps to reduce the energy use and enhance the integration of renewable energy installations. Built environment is attributed to 40% of the global energy use, and the literatures indicate that integrating the local renewable energy sources to the grid and meanwhile renovating the buildings can significantly improve the energy performance of building sector.

This thesis studies the energy performance and the potential to utilize solar energy and wind of a single-family house and an apartment block in Malmö, South Sweden. The case buildings were built in 1940s, with aged construction materials and building services system.

Through the study, it is noticed that the measured heating supply to the single-family house is not related to the weather and indoor activity. It can be inferred that there might be heating energy wasted and indoor discomfort. In high altitude countries like Sweden, it is possible for Photovoltaic panels facing East and West to have higher annual production than panels facing the South. Since the electricity flow between panels, grid and user is transient, most of the solar photovoltaic system is grid-connected distributed system.

Preface

I would like to express my gratitude to my supervisor Vahid Nik for the professional guidance and support throughout the study.

I would like to thank Patrik Thuring from E.ON. for helping me to collect the heating demand data of the case buildings.

Finally, I would also thank my friends and family for the advice and support.

Table of content

Abstract 2
Preface 3
Table of content 4
1 Introduction 6
1.1 Background 6
1.2 Research Questions and Objectives 6
1.3 Limitations 7
2 Literature Review 8
2.1 Renewable Energy Sources Utilization 8
2.2 Solar Energy 9
2.2.1 Solar Energy Potential 9
2.2.2 Photovoltaic panel 9
2.2.3 Solar Thermal Collector 10
2.3 Wind Energy 12
3 Methodology 16
3.1 Site Analysis 16
3.2 Software Description 18
3.3 Energy Performance Modeling 19
3.4 Renewable Energy Potential 21
3.4.1 Solar Energy 21
3.4.2 Wind Energy 22
4 Results and Analysis 24
4.1 Energy Performance Modeling 24
4.2 Solar Energy Installations 29
4.3 Wind Energy 36
5 Discussion 40
6 Conclusion 42
7 Summary 44
References 46
Appendix A. Construction material layers 51
Appendix B. Occupancy Schedule 54

1 Introduction

1.1 Background

With more convenience brought by the modern technology, the energy demand is increasing in all sectors. The building sector is attributed to approximately 40% of the global energy use and carbon emission (Makridou et al., 2016) and in North Europe region, heating accounts for up to 70% of the total energy use (Lee et al., 2017) while lighting accounts for 15%-50% in office buildings. However, these proportions can vary between one single building and another if the input is different, for example, the orientation, window-wall ratio and occupancy. Facing the global energy crisis, European Union requested that by the end of 2020, all the new buildings in member states should be near zero energy buildings (European Union, 2010). Malmö, where the case neighborhood is located, is the third largest city in Sweden and aims to completely run on renewable energy by 2030 (Faust, 2011).

In the building process, the orientation, thermal mass storage and HVAC schedule, etc. can be optimized to reduce the energy demand and put off the peak of demand. In the maintenance phase, advanced control system, such as absence sensor, can be applied to satisfy energy efficiency and thermal comfort at the same time. The Paris Agreement (2016) appeal to countries to improve the energy strategies on both demand and supply sides. Therefore, the role of buildings in the energy grid should not be simply the consumer but shifted to also the storage and generator of energy. After the large-scale power off in part of the United States and Canada in 2003, the concept of smart grid was put forward for the first time. The smart grid must integrate non-dispatchable renewable energy sources on the supply side and on-site energy supply from the demand side (Sioshansi, 2012). With the smart grid developed, more renewable energy and space on the building surfaces can be fully utilized, the possibility of large-scale power off will be lower and less money will be spent on grid construction. Malmö city requests that not only the buildings are designed to be low energy demand, the neighborhood will be powered with solar, wind energy and biofuels (Faust, 2011).

1.2 Research Questions and Objectives

The aim of the study is to assess the renewable energy potential of a residential neighborhood from 1940s in Malmö and then use the solar and wind energy as distributed energy sources, thereby changing the role of buildings from simply the consumer in the energy grid to the generator and making full use of the space in the built environment. The approaches to utilizing renewable energy sources should be further applied in similar residential neighborhood and under similar weather conditions.

The study was conducted to solve the following research questions:

1. How much is the energy demand of the case buildings from simulation?
2. How much is the energy production potential of solar energy installations and the wind turbine?

1.3 Limitations

The construction plans are scanned hand drawn plans, leading to minor inaccuracy of the thermal modeling. Only the hourly heating demand profile is provided to validate the energy simulation, and the electricity profile is missing due to the measuring system upgrade. Assumptions are made according to the ASHRAE guide and measured data. The weather file used for energy simulation is only for one year, in which the extreme weather conditions are not included.

2 Literature Review

2.1 Renewable Energy Sources Utilization

Malmö, located in Southern Sweden, is connected to Denmark with Öresund bridge. Western Harbor, Augustenborg and Sege Park are three pioneering neighborhoods in Malmö in terms of renewable energy installation. Western Harbor was originally a piece of industrial land, and Bo01 decided to turn the area into energy efficient residential neighborhood (Svekom, 2003). Around 1000 apartments are supplied with renewable energy sources including wind energy, solar photovoltaic, solar thermal and heat pump (Nilsson, 2007). The electricity is generated by large wind turbine in North Harbor, small rooftop turbines and photovoltaics, while the resources of heating are waste incineration, solar thermal collectors and thermal storage in the bedrocks (Malmo.se, 2016). There are 10 geothermal wells with temperature of approximately 10℃ all year around. Most part of the heat is delivered by the heat pump and cooling during summer is delivered to the office buildings outside the neighborhood (Urbangreenbluegrids.com, 2008). The solar thermal collectors are located on the roofs and façade, and connected to the district heating network, replacing the large storage tank with district heating network (Nilsson, 2007). In addition, the buildings built at later stages of the project are passive houses with lower energy demand.

In Augustenborg, solar thermal collectors are installed and connected to the central heating system. Photovoltaic panels and wind power plant are installed to generate electricity (Malmo.se, 2008). Electricity in Sege Park is from wind and photovoltaic and heating is from solar thermal and bioenergy (Malmo.se, 2016).

Distributed energy sources are the nearby units which supplies energy to the buildings and stores energy, including the renewable energy installations (Alanne and Saari, 2006). Microgrid is one of the most effective ways to integrate renewable energy in the energy grid, as it eliminates the negative effects of renewable energy sources and provides reliable power output (Wang et al., 2016).

2.2 Solar Energy

2.2.1 Solar Energy Potential

Several decades ago, the electricity was mainly supplied with central power plant, while nowadays there are more shares for renewable energy sources, which are highly dependent on the locations, such as, wind and solar energy (Resch et al., 2014). Direct normal radiation and global horizontal radiation can indicate the general distribution of solar energy sources, which is provided by Solargis, a solar radiation database and solar power software provider. Diffuse solar radiation is the part of solar radiation scattered by the atmosphere and reflected radiation is the part reflected by another surface first. A part of solar radiation can reach the surface directly, without being scatter and reflected, that is the direct radiation. The sum of the diffuse radiation, reflected radiation and direct radiation is the total radiation received on a surface, which is regarded when designing the photovoltaic and solar thermal system (Matejicek, 2017). The solar radiance map based on GIS is produced in three steps. First of all, the clear sky radiance is calculated, and then with the help of satellites, the effect of cloud is taken into consideration and direct normal radiance. The last step is to include the effect of the surroundings on the studied surface (Matejicek, 2017). The total solar radiation of earth surface is dependent on time and latitude (Earthobservatory.nasa.gov, n.d.). The solar radiation model is based on long term data and annual total radiation level can be used as reference for solar energy installations.

2.2.2 Photovoltaic panel

Electricity can be generated from solar energy either directly by photovoltaics (PV) or indirectly by large concentrated solar power plant (Matejicek, 2017). The solar energy is completely for free and the electricity generation process is free of noise and emission. The installed PV capacity in Sweden has been increasing sharply since 2010, especially the grid-connected distributed PV. By 2016, the total installed PV capacity in Sweden is over 200MW, and grid-connected distributed PV accounts for approximately 80% of it (Lindahl, 2016). In Spain, where the cooling load is high during summer, the cold thermal energy storage is applied to shift the cooling load peak time, and time-of-use tariff is used to achieve demand side control. Both strategies can be integrated with off-grid solar PV to reduce the annual electricity demand and shift the power peak (Saffari et al., 2018).

The energy source is highly dependent on the weather condition and the life cycle of PV panels may have an influence on the environment (Karlsson & Nilseng, 2016). The voltage and current of the electricity generated by PV depend on the amount of PV panels and how they are connected (PVEducation, 2018). An inverter is required for the system, as the electricity output is direct current. In the PV panel market in Sweden, the efficiency ranges from 7% to 20% and with one Celsius degree rise of temperature, the panel efficiency can drop by up to 0.45% (Karlsson & Nilseng, 2016).

There are three types of commonly installed PV cells, shown in Figure 1, mono crystalline silicon, poly crystalline silicon and thin film solar cells (Bernardo, 2017). The mono crystalline silicon solar cell is made of silicon ingots. In addition to the even and uniform look, it has higher efficiency, up to 21.5%, saves space and has longer life span than the other two, while its cost is also the highest. The poly crystalline silicon cell is made of melted raw silicon. The costs for both the material and the manufacture process are lower than mono crystalline silicon cell. However, its efficiency is between 13% and 16%. Thin film solar cells can be subdivided into Amorphous silicon (a-Si), Cadmium telluride (CdTe), Copper indium gallium selenide (CIS/CIGS) and Organic photovoltaic cells (OPC). Thin film solar cells are cheaper than crystalline based solar cells, but the efficiency is also lower. The uniform appearance gives it more chances to be integrated with building (Energy Informative, 2015).

Figure 1. mono crystalline, poly crystalline and thin film PV panels (Pickerel, 2015)

When designing the layout of the PV panels, shading from surroundings and mutual shading must be taken into consideration, since shadings will not only reduce the electricity output, but also create a hot spot and degradation of the panel (Pveducation.org, 2018). In Sweden, the optimal PV panel layout is 41° to 48° tilt and facing South (Sommerfeldt, Muyingo & af Klintberg, 2016). If the PV panels are tilted to achieve higher production, then the row distance should be increased to eliminate the effect of mutual shading. The optimal row distance can be calculated with software (Energytrust.org, 2009). For PV panels on the flat roof facing due South, when the tilt angle is approximately equal to the latitude, the panel has the maximum production and when the tils angle is 0°, the area has the maximum production (Kanters and Davidsson, 2014).

2.2.3 Solar Thermal Collector

There was 15% drop in the installation of solar thermal collectors from 2013 to 2014 (Weiss, Bergmann & Stelzer, 2009), and economic feasibility is the main reason why there is such a difference between the PV panel market and solar thermal collectors (Hang, Qu & Zhao, 2012). There are two main applications of solar thermal collectors, one is to cover the Domestic Hot Water (DHW) need and the other is for district heating purpose. Large scale solar heating plant, with more than $500m^2$ solar collectors, is the minor part of solar heating installation (Dalenbäck, 2005).

The building heating demand can be divided into space heating during winter time and constant DHW demand throughout the year. If the solar thermal system is sized for the highest demand, the sum of space heating and DHW, then during summer time when the solar radiation is significantly higher, the liquid in the collector can be boiling and reach the stagnation phase. The liquid in the collector will start to evaporate when the temperature rises to the boiling point, and then the liquid will be pushed into the expansion vessel (Hausner and Fink, 2002). If the solar radiation remains at high level, the absorber will be emptied by the superheated steam, until the solar radiation level drops and the absorber temperature is lower than the boiling point, the steam will condense and flow back to the collector. Therefore, the solar heating system should be sized to only meet the DHW demand and district heating or electrical heater can be the auxiliary heating source (Davidsson, 2017). Previous studies on the thermal storage tank shows that in 15℃ temperature range in the thermal storage tank and volume of 0.01 ~ 0.02 m^3/m^2 collector area would be the most efficient in terms of thermal storage (Li et al., 2015). The solar fraction of such system in South Sweden can reach 50% and the payback period is around 17 years (Bernardo, Davidsson and Andersson, 2016).

There are three main types of solar collectors, evacuated tube collector, flat plate collector and plastic absorber (Davidsson, 2017). The performance of the solar collector follows equation (1):

$$q = K_b \cdot F' \cdot (\tau\alpha)_n \cdot G_b + K_d \cdot F' \cdot (\tau\alpha)_n \cdot G_d + K_g \cdot F' \cdot (\tau\alpha)_n \cdot G_g - F' \cdot \Delta T \cdot U_1 - F' \cdot \Delta T^2 \cdot U_2 \qquad (1)$$

Where, K is the coefficient for incidence angle, F' is coefficient for heat loss from fins, $(\tau\alpha)_n$ describes how much radiation can be absorbed for 0° incidence angle, G is the solar radiation, ΔT is the temperature difference between liquid and the ambient and U is the heat loss coefficeint.

The coefficients K, $(\tau\alpha)_n$, F′ and U indicate the properties of the materials and therefore suggest the performance of the solar collectors. For high temperature applications, such as DHW, the temperature between working fluid and the ambient air is high and better insulation, high U-value, is required (Iparraguirre et al., 2016). For pool heating, the unglazed collectors are often used (Kalogirou, 2004).

2.3 Wind Energy

The working period of solar energy installations is limited to daytime, so for residential buildings the supply and demand occur at different period, while wind turbines can generate electricity during night time (Bahaj, Myers and James, 2007). The output of one coal power plant is equal to the output of hundreds of wind power plants (Matejicek, 2017). In remote region, where there is no electricity grid connection and the wind velocity is high, the wind power is especially beneficial. It is recommended that if the average wind velocity is higher than 6.5m/s, an onshore wind turbine can be installed and 3 – 10 rotor diameters spacing is suggested for the turbine to acquire energy (Matejicek, 2017). The power output from a wind turbine follows equation $P= 0.59 \cdot \frac{1}{2} \cdot A \cdot \rho \cdot v^3$ (2):

$$P = 0.59 \cdot \frac{1}{2} \cdot A \cdot \rho \cdot v^3 \quad (2)$$

Where A is the area, ρ is the air density and v is the air velocity.

Since the power output is proportional to the cube of air velocity, it is highly unstable. The maximum efficiency possible for wind turbine is 0.59, the Betz limit, resulted from the rest of the energy carried by the wind downstream, and the actual wind turbine efficiency ranges from 35% to 45% (Hanania, Stenhouse and Donev, 2018). In Europe, apart from the global GIS based resource maps from ArcGIS, wind resource maps are provided by companies, for example, windNavigator from AWS Truepower (Matejicek, 2017).

However, the Life Cycle Assessment (LCA) of wind turbine shows that the Global Warming Potential of wind power is 4.6 to 26 gCO_2/kWh (Matejicek, 2017). The high level of Carbon emission is mainly caused by concrete foundation of wind turbines. Since the velocity of wind downstream is considerably reduced, the effect of wind turbine on the surrounding eco system remains uncertain.

The wind profile in built environment tends to be more turbulent, since the buildings and vegetation are the obstacles (Eliasson et al., 2006). Micro-scale wind turbines installed in built environment are emerging in the European market. Horizontal axis wind turbines (HAWTs) and Vertical axis wind turbines (VAWTs) are two types of mainly used turbines (Chen, Guerrero and Blaabjerg, 2009), indicated in Figure 3 and Figure 4. Table 1 shows the difference between two types of turbines. For the built environment turbine to function well on rooftop level, the cut-in wind velocity should be 1.2 m/s, which has not been available in the market. Otherwise, the recommended height for built environment wind turbine is 15m (Manyeredzi and Makaka, 2018). As the micro wind turbines are installed in a residential neighborhood, more aspects should be taken into consideration, including the noise level, cut in wind velocity and whether it is safe to people and animals (Müller, Jentsch and Stoddart, 2009). For the newly designed buildings, the BIPvWt system (see Figure 2) can be used as building façade, and the 44.8% of the heating load and cooling load was eliminated by reducing the window wall ratio from 100% to 30% (Lee et al., 2017).

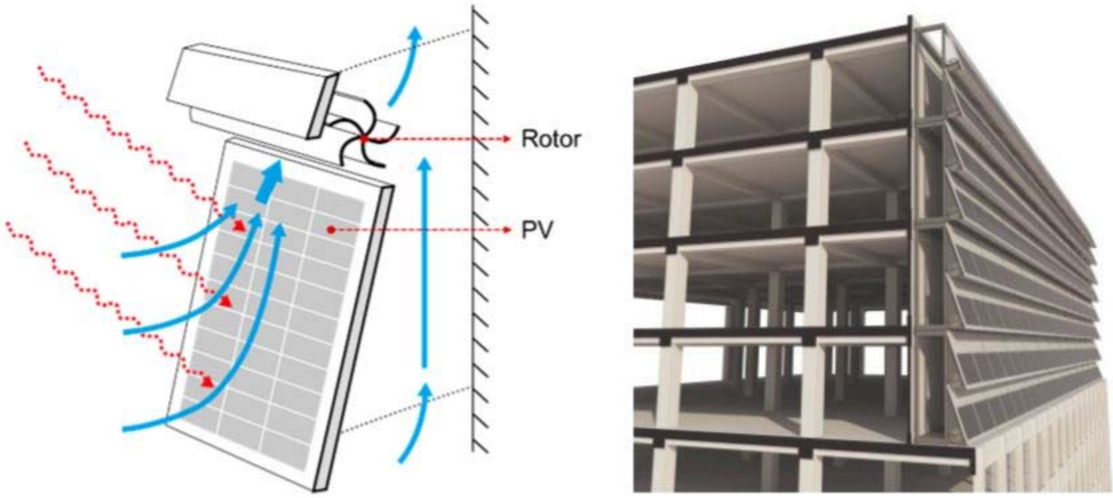

Figure 2. Design concept and building integration of the BIPvWt proposed by Lee et al (2017)

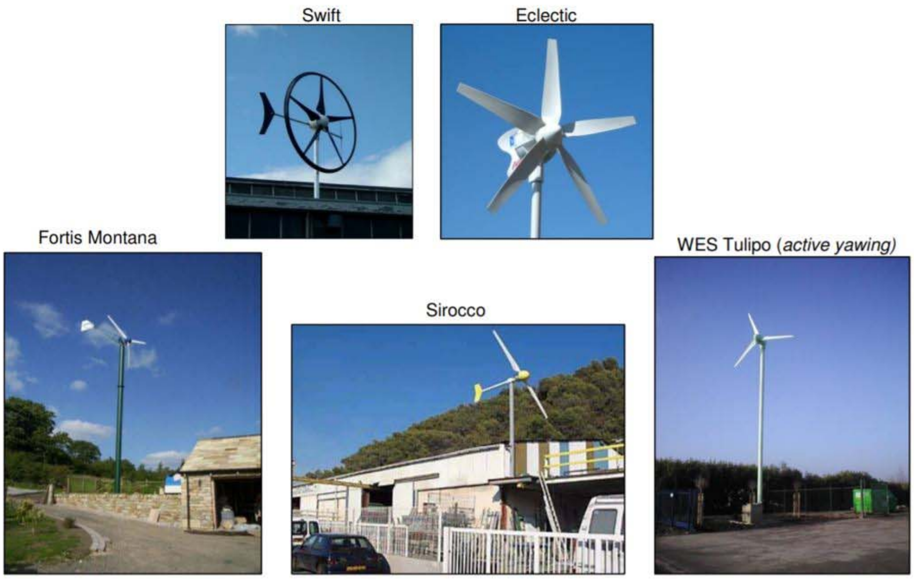

Figure 3. Existing models of HAWT (Cace et al., 2007)

Figure 4. Existing models of VAWT (Cace et al., 2007)

Table 1. Comparison between HAWT and VAWT (Ishugah et al., 2014)

	HAWT	**VAWT**
Direction	Into the wind direction	Not specified
Overall efficiency	High	Low
Effect of wind direction and turbulence	Lower performance	Few effect
Best location	Open area where there is no obstacle	Built environment

3 Methodology

3.1 Site Analysis

Sofielund, surrounded by Ystadvägen, Lantmannagatan, Lönngatan and Nobelvägen, is the object of the performed study. Sofielund is located in between of Malmö city center and suburb area, and a train station will be built in one year. As can be seen in Figure 5, it is a residential neighborhood, with a mix of three to four floors apartment building blocks, single family houses and grocery stores. In order to estimate check the potential of installing solar thermal collectors, PV panels and micro wind turbines, the solar radiation and wind velocity of the area are studied either with GIS based maps or through weather file plotted with Ladybug.

According to the construction plan, the residential buildings in the neighborhood are designed and built in 1940s. One single family house and one apartment block, shown in Figure 6, are selected to conduct the thermal modeling and solar energy potential. There is no open space to place the solar thermal collectors or PV panels on the ground and for the wind to rise to high velocity. There are no high-rise buildings in the neighborhood and the height of vegetation is relatively low, which is suitable for harvesting solar energy on the roof.

The Southeast roof area of the single family house is 58m^2 and the roof angle is 27°. Table 2 shows the area, tilt and azimuth of every part of the roof of the apartment block, measured with Google Earth.

Table 2. Area, tilt angle and azimuth of each part of the roof

Roof part	Area [m^2]	Tilt angle [°]	Azimuth [°]
A	299	27	196
B	499	27	288
C	299	27	12
D	508	27	103
E	81	32	16
F	417	32	108
G	209	32	192
H	372	32	273

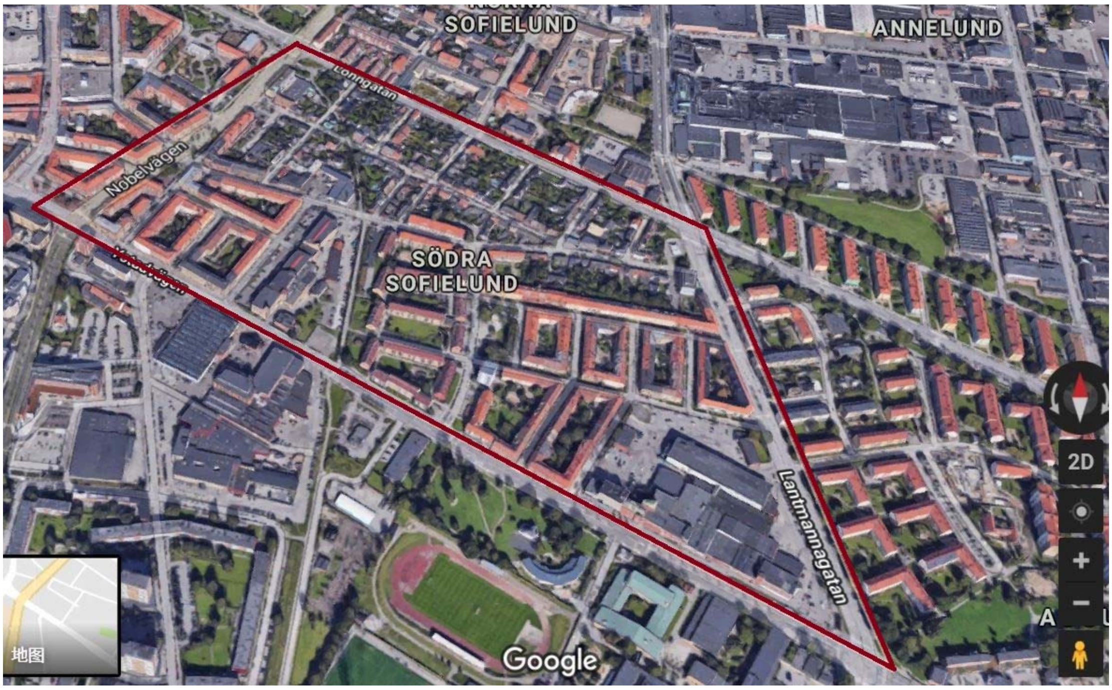

Figure 5. Sofielund neighborhood

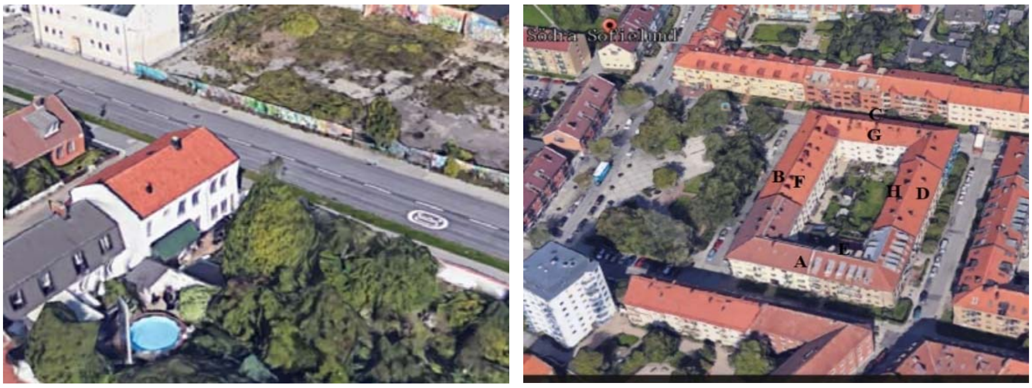

(a) (b)

Figure 6. Sample buildings from google map

3.2 Software Description

AutoCAD: a software to draw and draft 2D design and export to 3D design software in DWG format (Autodesk.com, 2018).

Rhinoceros: a computer aided design software, in which users can model 3D objects with different sizes, render, animate and analyze (Rhino3d.com, 2018).

Grasshopper: a plugin for Rhinoceros, using script to edit the model or graphics in Rhinoceros (Grasshopper3d.com, 2018). In this case, Archsim is used to simulate the thermal performance of buildings.

Ladybug: a plugin for Rhinoceros, where environmental design is conducted and weather data is analyzed (Grasshopper3d.com, 2018).

Ecotect: a software to analyze the weather data and building energy performance (Autodesk.com, 2018).

System Advisor Model (SAM): a software where the solar energy installations are simulated, in the aspects of performance and finance (Sam.nrel.gov, 2018).

Autodesk Flow Design: a software to simulate the wind velocity and pressure around the obstacles (Autodesk.com, 2018).

3.3 Energy Performance Modeling

As can be seen in Figure 7, one single family house and one apartment block are selected as the sample buildings to do energy simulation and the model is shown in Figure 8. After the construction plans are collected from Malmö municipality, the buildings are modeled in Rhino (see Figure 8). The architecture plans, construction material and room functions are included in the construction plans, and the thermal zones are divided according to the room functions. The weather file for Copenhagen is used, due to the lack of weather file in Malmö and the negligible distance between two cities. The occupancy density and internal gains are assumed according to ASHRAE 62.1 (2010) and ASHRAE 90.1 (2013). The internal gain from occupants is determined by both occupancy density and occupancy schedule. Occupancy density is the value when the room is occupied and the percentage of occupancy changes, indicated in Appendix B. The occupancy schedules are assumed according to the room function from the construction plans. The hourly heating energy demand profiles are requested from the energy company E.ON., and used to compare with simulation results and then to calibrate the settings. The occupancy schedule is approximated and then the electricity and DHW demand profile can be determined, for sizing the renewable energy installations. The electricity and heating demand of the whole neighborhood is determined by scaling the results from the sample buildings with the area and number of buildings.

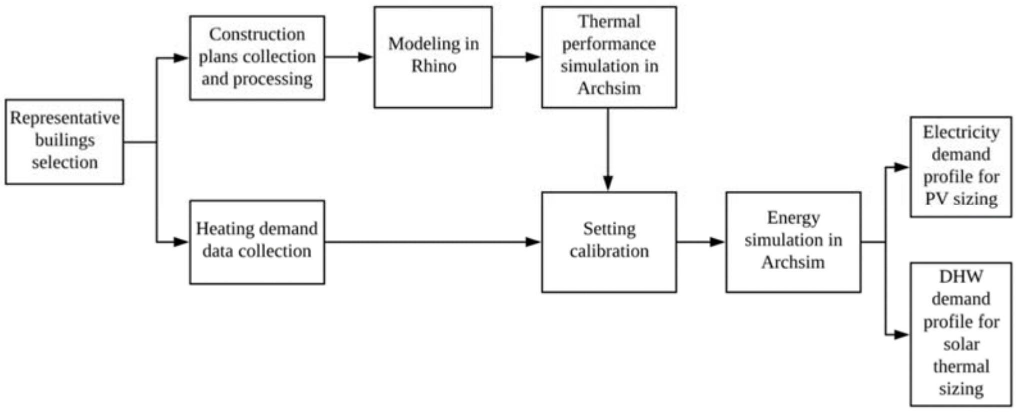

Figure 7. Work flow of the energy performance modeling

Table 3. U-values of the building envelopes

	Single family house	Apartment block
External wall	0.245	0.245
Roof	1.015	0.12
Internal wall	2.422	0.247
Floor	2.422	2.258
Foundation	1.112	1.018

When calibrating the thermal performance simulation according to the measured heating profile, the occupancy density, heating set point and infiltration rate were three main parameters adjusted, see Table 4 and Table 5.

Table 4. Settings for the single-family house during calibration process

	Zone name	Case 1	Case 2	Case 3	Case 4
Occupancy density [p/m^2]	**Living room**	0.03	0.03	0.03	0.03
	Bed room	0.03	0.03	0.03	0.03
	Kitchen	0.03	0.05	0.05	0.05
	Bathroom	0.03	0.06	0.06	0.06
	Corridor	0.03	0.03	0.03	0.03
	Storage	0.03	0.02	0.02	0.02
Heating set point [℃]		22	22	21	21
Infiltration rate [ACH]		0.1	0.1	0.1	0.2

Table 5. Settings for the apartment block during calibration process

	Zone name	Case 1	Case 2	Case 3	Case 4
Occupancy density [p/m^2]	**Office**	0.03	0.05	0.05	0.05
	Bed room	0.03	0.05	0.05	0.05
	Kitchen	0.03	0.1	0.1	0.1
	Bathroom	0.03	0.08	0.08	0.08
	Circulation	0.03	0.1	0.1	0.1
	Storage	0.03	0	0	0
Heating set point [℃]		21	21	23	23
Infiltration rate [ACH]		0.1	0.1	0.1	0.3

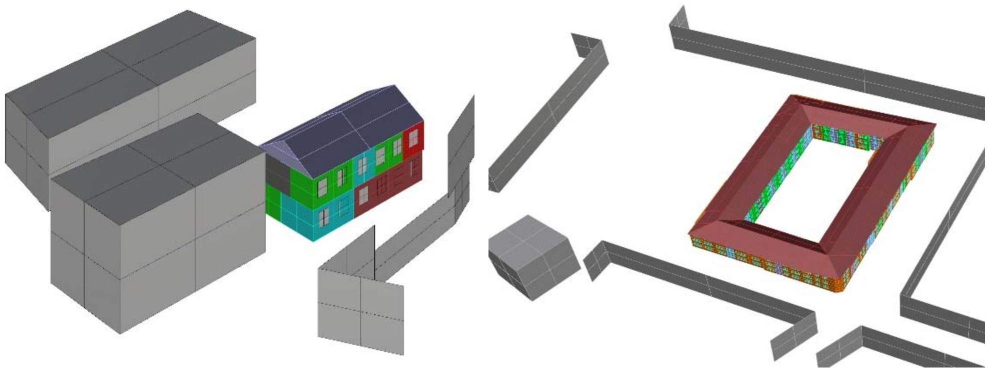

(a) (b)

Figure 8. Simulation models of the single-family house (a) and apartment block (b)

3.4 Renewable Energy Potential

3.4.1 Solar Energy

In order to determine the proper location of the PV panels and solar thermal collectors, annual solar radiation and shading analysis are conducted to the building surfaces including roofs and facades. Since the PV panels are more sensitive to the shadings than the solar thermal collectors, the locations to place PV panels are selected first. The PV panels will be installed on residential buildings, therefore only monocrystalline and polycrystalline PV panels are compared, with detailed parameters indicated in Table 6.

Table 6. Parameters of two compared PV panel models

	LG350Q1K-A5	**TalesunTP660P-260**
Type	Monocrystalline	Polycrystalline
Nominal efficiency [%]	21.1	16
Max power [W]	353	260
Max power voltage [V]	36.2	30.6
Max power current [A]	9.8	8.5
Open circuit voltage [V]	42.7	37.7
Short circuit current [A]	10.8	8.9
Module length [m]	1.67	1.62
Module width [m]	1	1

Because the PV panels are installed on a pitched roof, the tilt angle will be the same as roof angle and the row distance will be zero. The overproduction from the PV panels will be sold to the energy company, so from the occupants' stand, the PV system is sized with the hourly electricity demand, obtained from the energy simulation. Two types of PV systems are compared, hourly demand coverage, with minimum amount of electricity sold to the energy company, and whole roof system, where the buildings are also the generator in the energy grid. Afterwards, the array of PV panels is simulated in SAM to include the losses from the inverter and the system.

Similar to the PV panels, the tilt angle and row distance of the solar thermal collectors will be roof angle and zero respectively. Theoretically the water heated by the solar thermal collectors can be used for DHW and space heating. However, the daily solar radiation is relatively low during the heating season, while the DHW demand remains constant throughout the year. To avoid liquid boiling in the absorber during summer, the solar thermal collectors are sized to meet the DHW demand, and the space heating is supplied with district heating. DHW requires high water temperature, so a glazed flat plate solar collector with good insulation is selected and the properties are shown in Table 7. The tank size is adjusted to be suitable for certain number of solar collectors.

Table 7. Parameters of the selected solar thermal collector

Model	**Area [m^2]**	**IAM**	**FRta**	**FRUL**
Vaillant Solar Systems VFK 150 H	2.51	0.09	0.775	2.43

IAM is Incidence Angle Modifier and higher IAM means that the effect of solar incidence angle is less. FRta is the optical gain and higher FRta means more solar radiation is absorbed by the solar collector. FRUL is the thermal loss coefficient and lower means better insulation (Blair et al., 2014).

3.4.2 Wind Energy

In order to assess the wind energy potential in the neighborhood, the wind from the weather data is first analyzed with Ecotect, including the velocity and direction. The wind tunnel simulation is conducted under the prevailing wind condition in Autodesk Flow Design. The location with high wind velocity can be identified from the simulation results and wind turbines are selected. Micro vertical axis wind turbines from Windside are applicable in the neighborhood. Figure 9 from left to right indicates the real-life installations of WS-12 in a shopping mall in Raisio, Finland, WS-4 in University of Vaasa, Finland and WS-4 in Brostol, the UK. Table 8 shows the parameters and applications of different models from Windside. In the end, the annual electricity output can be estimated from the product catalogues.

Figure 9. WS-12, WS-4 and WS-4 from Windside (Windside.com, 2018)

Table 8. Parameters of the VAWT models from Windside (Windside.com, 2018)

	Cut-in wind velocity [m/s]	**Wind endurance [m/s]**	**Max output [W]**	**Weight [kg]**	**Height [m]**	**Application**
WS-0,60City	Varies	20	162@12Vdc 259@24Vdc	59	2.3	Lighthouses, boats, park and street lights, and building-integrated/mounted.
WS-2CityG	2	25	375@12Vdc 450@24Vdc	210	2.8	Low wind speed areas, especially for urban environments.

WS-4	Varies	40	540@12Vdc 630@24Vdc	800	5	Highly visible installations in populated urban areas.
WS-12	2	40	-	4600	8	Chaotic wind environments

4 Results and Analysis

4.1 Energy Performance Modeling

The cumulative hourly heating demand profiles of the single-family house and apartment block, from simulation and measurement are shown in Figure 10 and Figure 11. The measured heating supply indicates that heating to the single-family house is divided into three periods and does not vary with the environment. The settings on occupancy, heating setpoint and infiltration rate are calibrated to reach the similar results with the measurement, for further simulation purpose. The annual heating energy is 19511 kWh and the total floor area of the single-family house is 176 m^2, so its heating demand is 109.7 kWh/m^2. Similarly, the total floor area of the apartment block is 7674 m^2, so the heating demand is 144.8 kWh/ m^2. The specific energy uses for both single family house and the apartment block are significantly higher than the Boverket requirement for dwellings with non-electric heating, 90 kWh/m^2 (BBR, 2011). The high heating energy demand can also be suggested by the high U-values of the building envelope shown in Table 3.

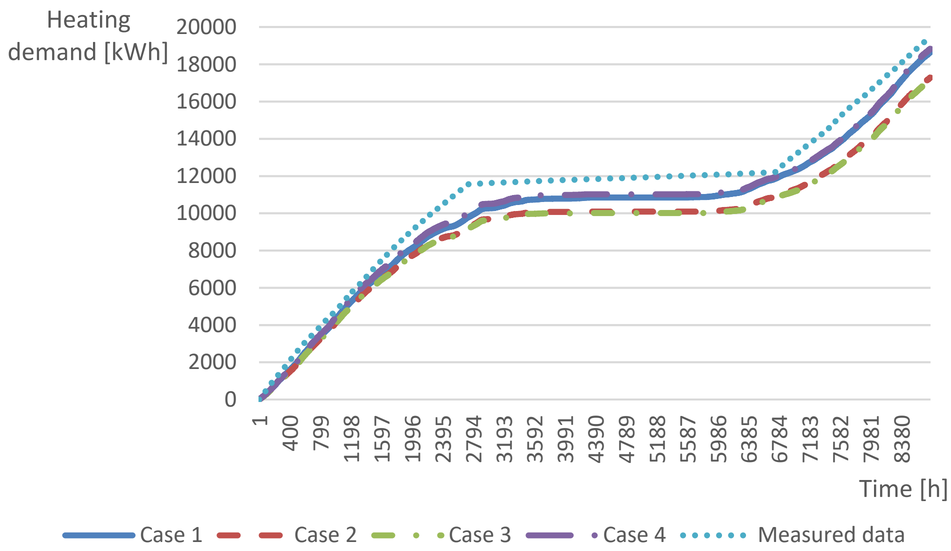

Figure 10. Simulation and measured heating profile of the single-family house (cumulative)

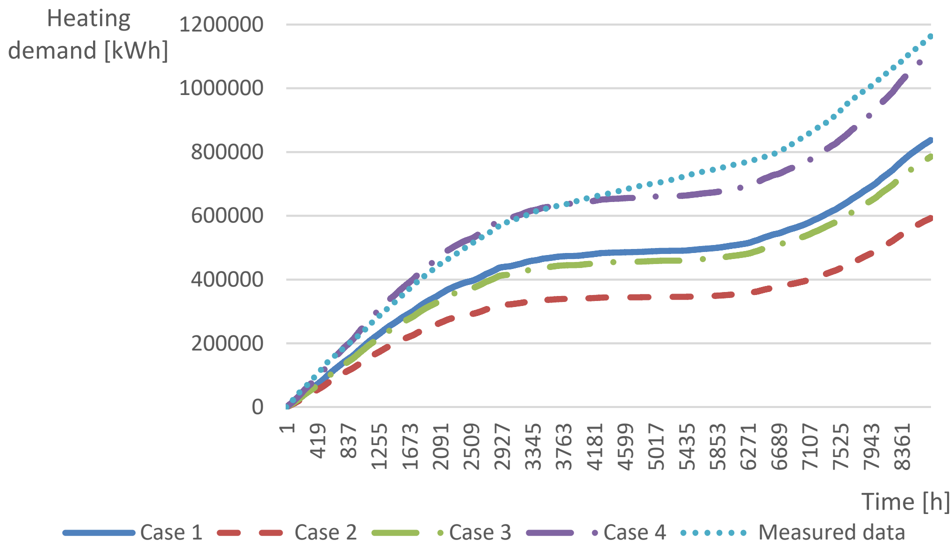

Figure 11. Simulation and measured heating profile of the apartment block (cumulative)

As can be seen from the measured heating supply in Figure 12, that in a week during heating season, the hourly supply to the single-family house fluctuates around 5 kWh, and it does not vary with the occupancy schedule, suggesting that there is no thermostat to automatically control the indoor temperature. It is recommended that a setback thermostat can be applied to the heating system, and then the heating demand can be reduced during unoccupied hours. On the opposite, for the apartment block, it is obvious that there are seven peaks of heating energy supply in one week, indicating that internal heat gain and the environment are considered and probably there are thermostats on the heating system.

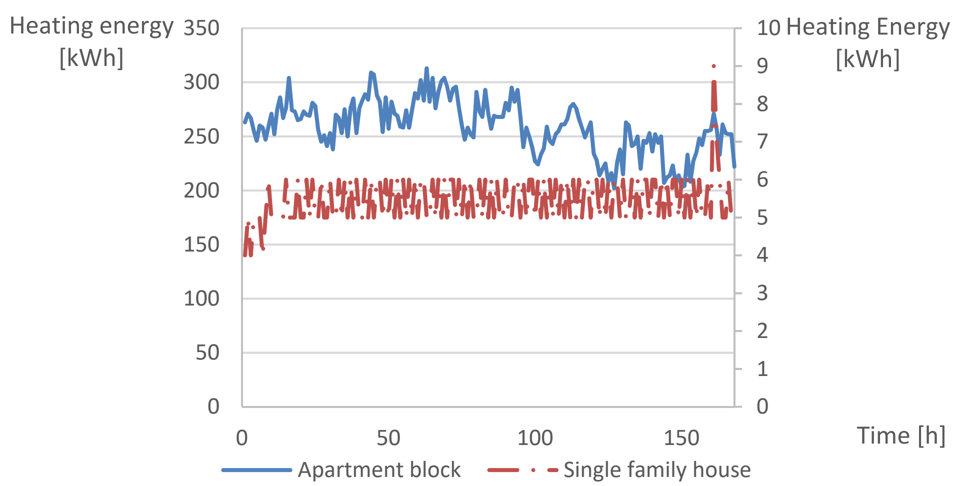

Figure 12. Measured hourly heating supply to the single-family house and the apartment block in a week

The heating energy demand of the buildings consists of space heating and DHW, and the monthly total heating energy and DHW are indicated in

Figure 13 and Figure 14. The electricity demand during winter is considerably higher than summer, shown in Figure 15, probably due to the shorter sunlight hours therefore more artificial lighting and the decorative lighting during Christmas and new year. However, the solar radiation level and electricity production from PV panels are also low during winter, so the supply peak and demand peak during a year do not match. Whereas in Southern part of Europe, such as Spain and Greece, where air conditioning is necessary during summer, the high electricity demand should also happen in summer. The annual electricity demand of the single-family house and the apartment block are 3816 kWh and 142859 kWh, leading to specific electricity use of 21.7 kWh/m^2 and 18.6 kWh/m^2. From occupants' point of view, in order to minimize the overproduced electricity sold to the grid, the PV system should be only enough to cover the minimum hourly electricity demand during PV function period, which is approximately 0.5 kWh and 25 kWh for the single family house and the apartment block respectively (see Figure 16 and Figure 17). Figure 18 and Figure 19 show the electricity demand variation of the house and the apartment block for each month.

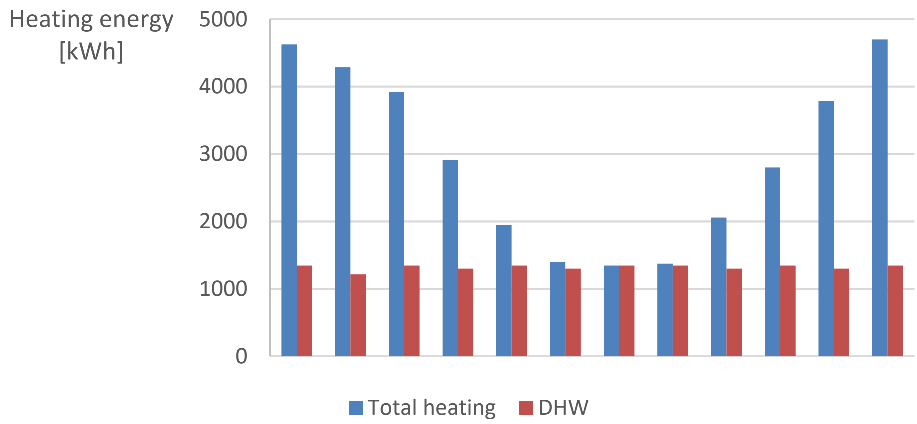

Figure 13. Monthly total heating energy and DHW heating energy of the single-family house

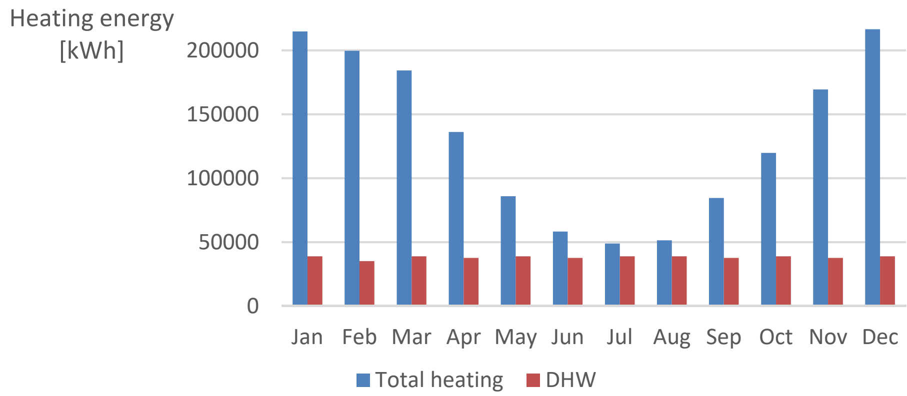

Figure 14. Monthly total heating energy and DHW heating energy of the apartment block

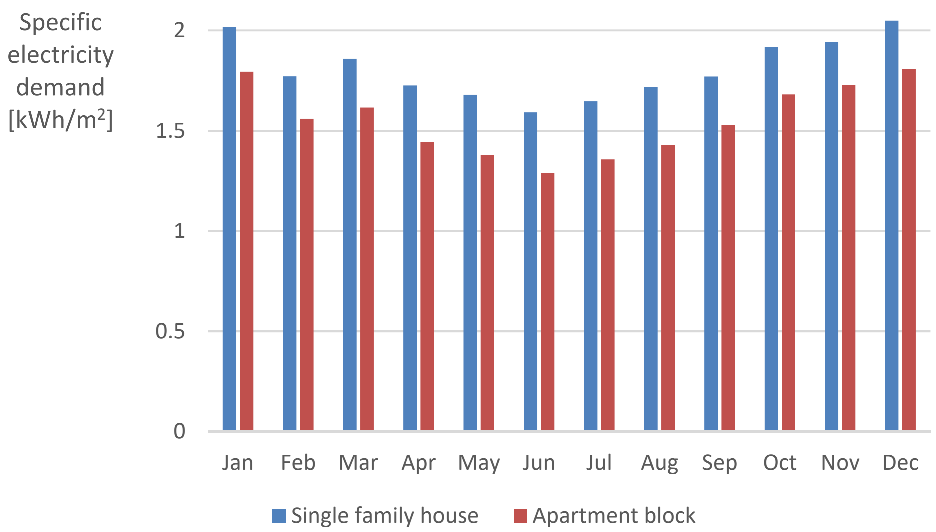

Figure 15. Monthly specific electricity demand profiles from the simulation

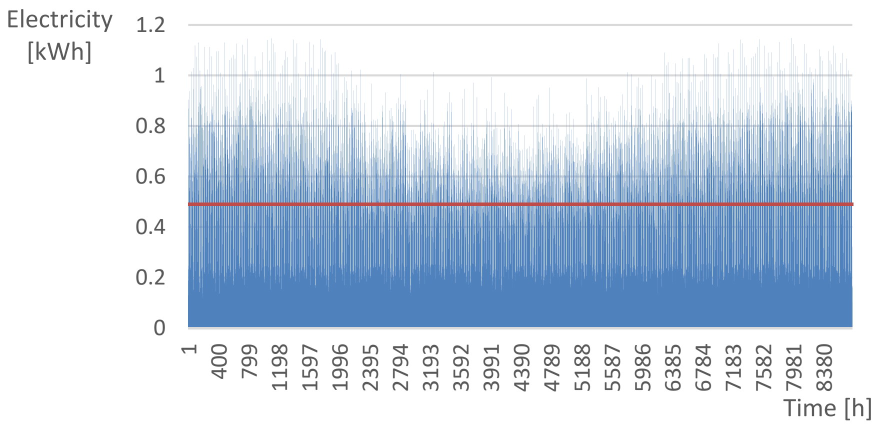

Figure 16. Hourly electricity demand profile of the single-family house

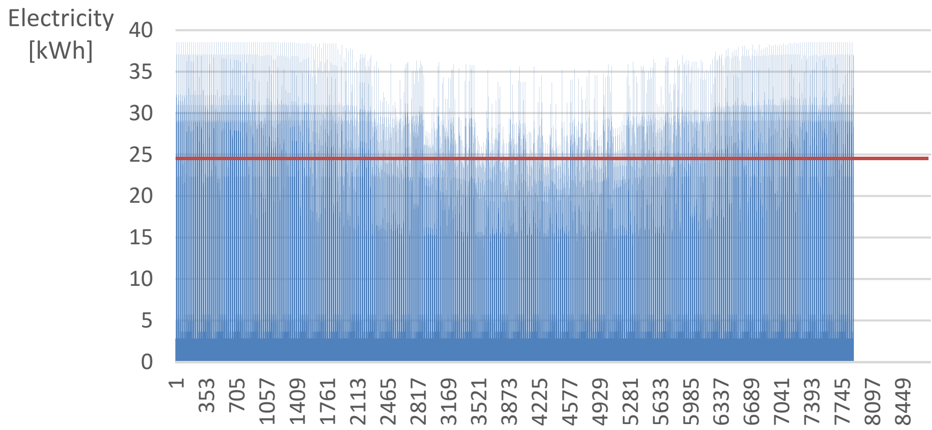

Figure 17. Hourly electricity demand profile of the apartment block

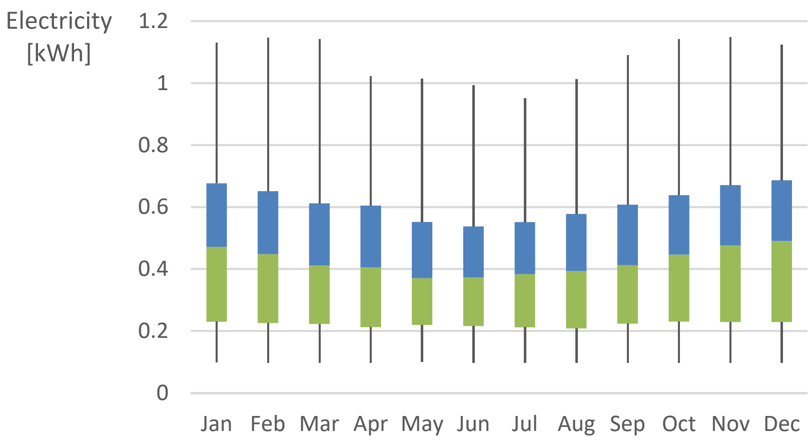

Figure 18. Electricity demand variation of the single-family house

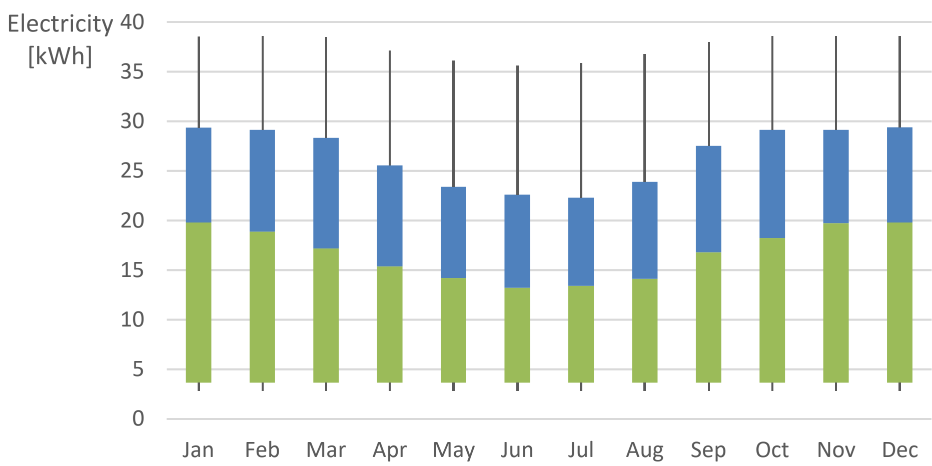

Figure 19. Electricity demand variation of the apartment block

4.2 Solar Energy Installations

The annual solar radiation and shadow range on the surfaces of the single family house are indicated in Figure 20. The annual radiation level on Southeast roof is over 1037 kWh/m^2 and is suitable for PV panels. The annual sunlight hour on the Southeast roof is high, as the house is surrounded by buildings with similar height. The vegetation in front of the house is projecting shading on the roof when the sun is low and the sunlight hour of the roof corner is slightly lower than the center. As a result, the plan is to place the solar thermal collectors on the East part of the roof and PV panels on the West part.

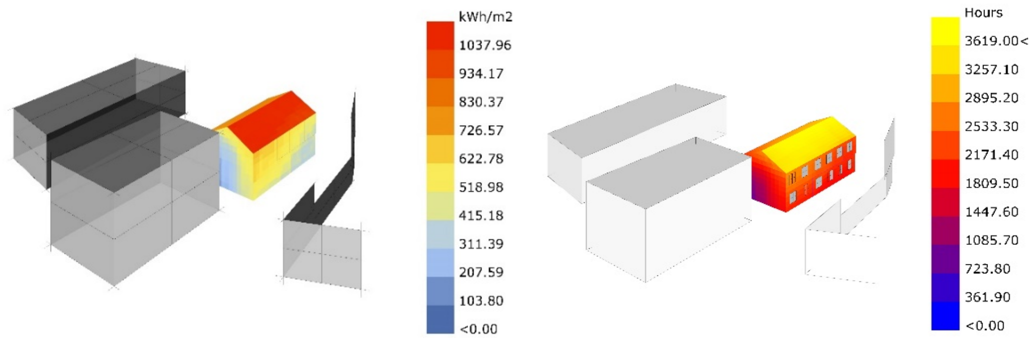

(a) (b)

Figure 20. Annual solar radiation analysis (a) and shadow analysis (b) of the single family house

As for the apartment block, the solar radiation levels on the roofs are all over 900 kWh/m^2 except for part C and part E facing the North. Roof part A and part G are receiving more than 1000 kWh/m^2 solar radiation each year and the sunlight hour is also higher than other parts of the roof (see Figure 21). The solar thermal collectors are installed on part F and part H, facing the yard and the PV panels are first placed on part A and G with the highest solar radiation and sunlight hours. During the summer in Sweden, the sun azimuth ranges from 48° to 312° (Solar Electricity Handbook, 2017), therefore the surfaces facing East and West can still receive considerable amount of solar radiation. In high latitude area, East-West system matches the electricity demand better and can reduce the load on the roof (Svensksolenergi.se, 2015). If more space is required, then the PV panels will be placed on roof part B and part D.

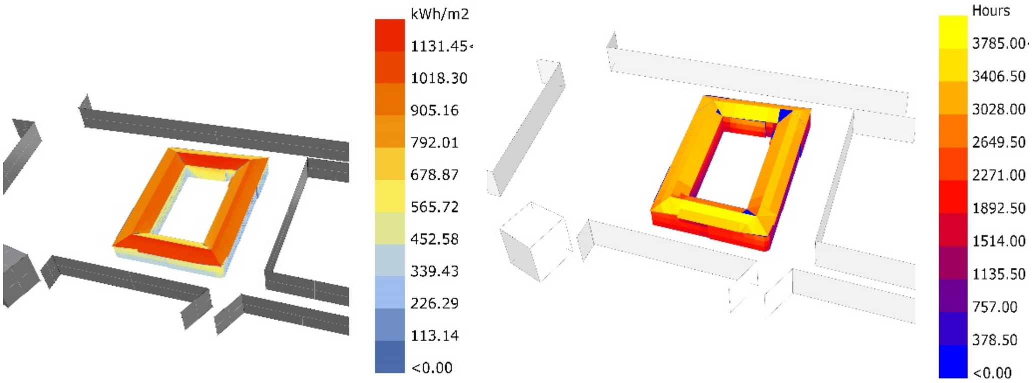

(a) (b)

Figure 21. Annual solar radiation analysis (a) and shadow analysis (b) of the apartment block

Ten solar thermal collectors are installed on the roof of the single family house, using 25.1 m^2 and the tank size is determined to be 1 m^3. With the collectors installed, 63% of the annual heating energy on DHW is covered by the solar energy and 4330 kWh needs to be supplied with auxiliary heating sources, such as electrical heater and district heating, shown in Figure 22. There is a considerable difference between the heating supply from solar collectors during summer and winter. Apart from the fact that the sun is low during winter, the 27° roof angle leads to large solar incidence angle and if the collectors are installed on roofs with larger tilt, then the supply gap between summer and winter should be smaller. In terms of space heating, large scale solar thermal power plant can convert solar radiation to heat and supply it with the district heating network (Winterscheid, Dalenbäck and Holler, 2017). For the apartment block, there are 130 solar thermal collectors on roof part F and roof part H, occupying 652.6 m^2 and the tank size is 80 m^3 in total. The solar fraction of the collectors is 47.7%.

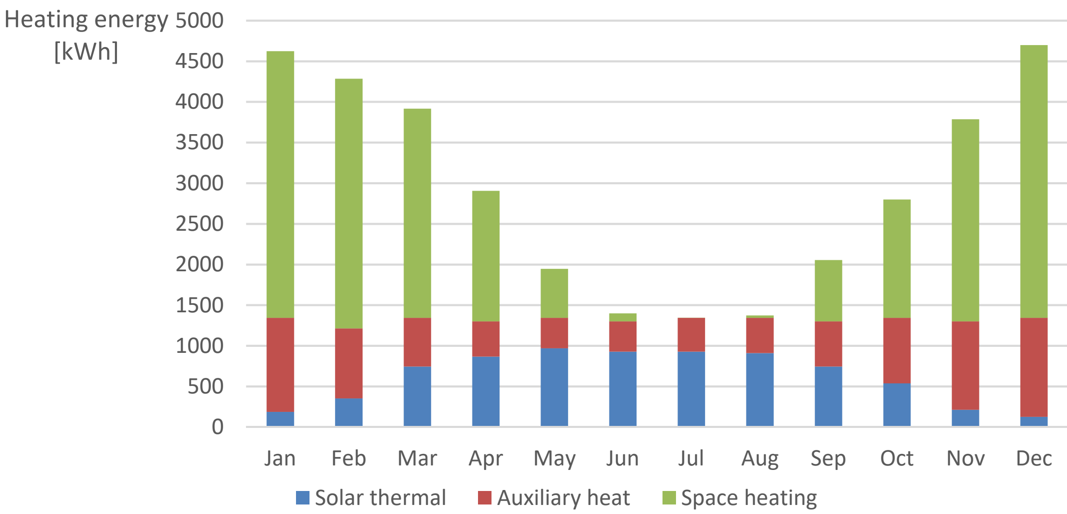

Figure 22. Monthly heating demand and heating resources of the single family house

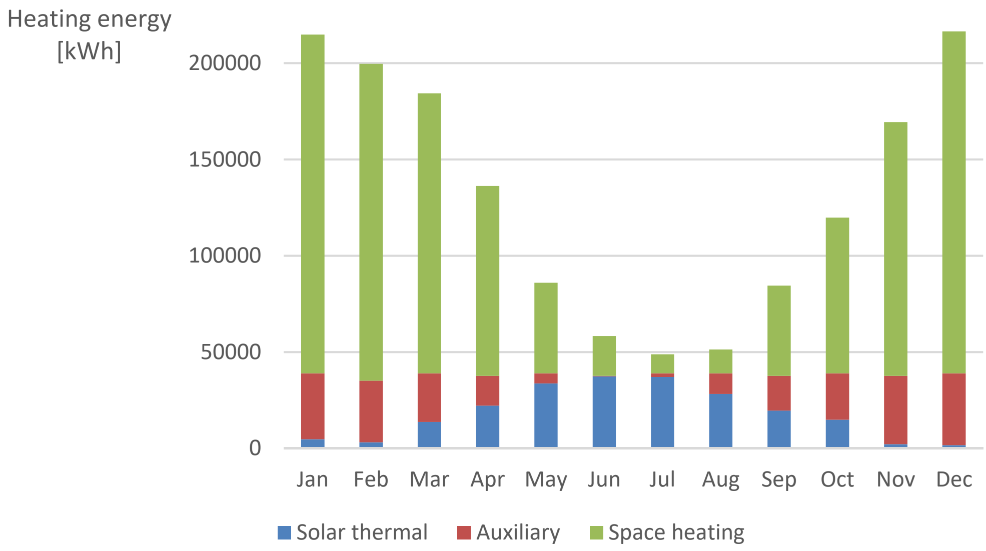

Figure 23. Monthly heating demand and heating resources of the apartment block

From the occupants' point of view, the lowest hourly electricity demand during the PV panel function period is 0.5 kWh and the sized system details with monocrystalline panels and polycrystalline panels are shown in Table 9. Figure 24 shows that monocrystalline and polycrystalline PV panels can both cover approximately 25% of the electricity demand. The annual energy supply nameplate capacity of the polycrystalline panel is approximately the same, but one more piece of polycrystalline panel and more space is required.

Table 9. PV system sizing results for the single-family house (occupants point of view)

	Monocrystalline	**Polycrystalline**
Modules per string	3	4
Strings	1	1
Annual energy supply [kWh]	962	961
Annual energy bought from the grid [kWh]	3056	3053
Annual energy sold to the grid [kWh]	202	197.7
Total module area [m^2]	5	6.5
Nameplate capacity [kWdc]	1.059	1.042
Inverter model	Ningbo Jinlong GCI-1K2G-H-US 208V	Ningbo Jinlong GCI-1K2G-H-US 208V

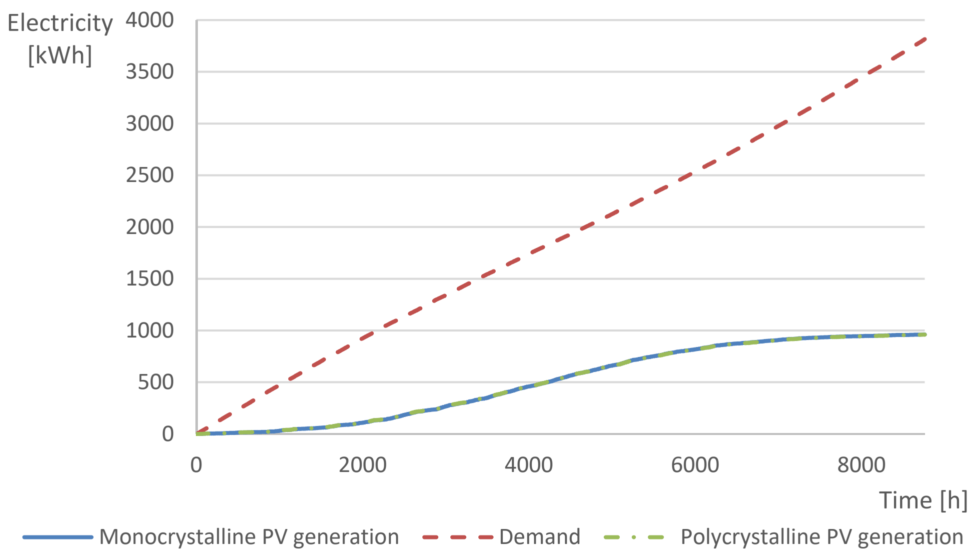

Figure 24. Cumulative electricity demand, monocrystalline and polycrystalline PV generation of the single-family house (occupants point of view)

From the energy company point of view, the whole roof should be covered with PV panels and the extra electricity goes to the grid. On the Southeast-facing roof, there is 33 m^2 space left to install the PV panels, besides the solar thermal collectors. As can be seen in Figure 25 and Table 10 that within limited space, monocrystalline generates more electricity and more overproduced electricity can be sold to the grid.

Table 10. PV system sizing results for the single-family house (energy company point of view)

	Monocrystalline	**Polycrystalline**
Modules per string	9	10
Strings	2	2
Annual energy supply [kWh]	5842	4900
Annual energy sold to the occupants [kWh]	2230	2322
Annual energy bought from the occupants [kWh]	4256.5	3406.7
Total module area [m^2]	30.1	32.5
Nameplate capacity [kWdc]	6.353	5.202
Inverter model	Growatt 7000MTLP-US 208V	Solectria PVI-5200TL 240V

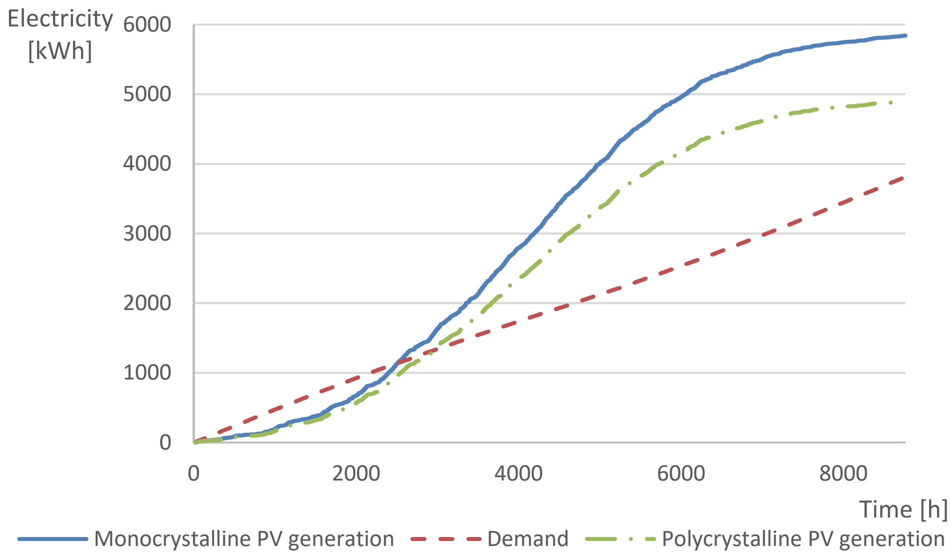

Figure 25. Cumulative electricity demand, monocrystalline and polycrystalline PV generation of the single-family house (energy company point of view)

For the apartment block, the PV system is designed to cover 25 kWh of hourly electricity use in order to not overproduce, and the annual electricity demand covered by PV system is 23.5%. Similar to the results of the single-family house, the monocrystalline PV system can produce same amount of electricity but the occupied space is smaller. For the roof parts facing East or West, fewer inverter can be used, since the panels can never reach their maximum capacity. The annual monocrystalline PV system generation is 60% higher than the actual demand and the polycrystalline system generation is 30% higher, indicated in Figure 27. Since the electricity flow between the consumer and the grid is transient, no matter how large the PV system is, there is always electricity bought from the grid, unless a battery is used to store the electricity generated by PV for several days.

Table 11. PV system sizing results for the apartment block (occupants point of view)

	Monocrystalline	**Polycrystalline**
Location	Roof part A	Roof part A
Modules per string	17	17
Strings	6	8
Number of inverters	6	3
Annual energy supply [kWh]	33637	33571
Annual energy bought from the grid [kWh]	114974	114638
Annual energy sold to the grid [kWh]	5562	5354
Total module area [m^2]	170.6	220.9
Nameplate capacity [kWdc]	36	35.4
Inverter model	Ningbo Jinlong Solis-6K-US 480V	Fronius Primo 11.4-1 240V

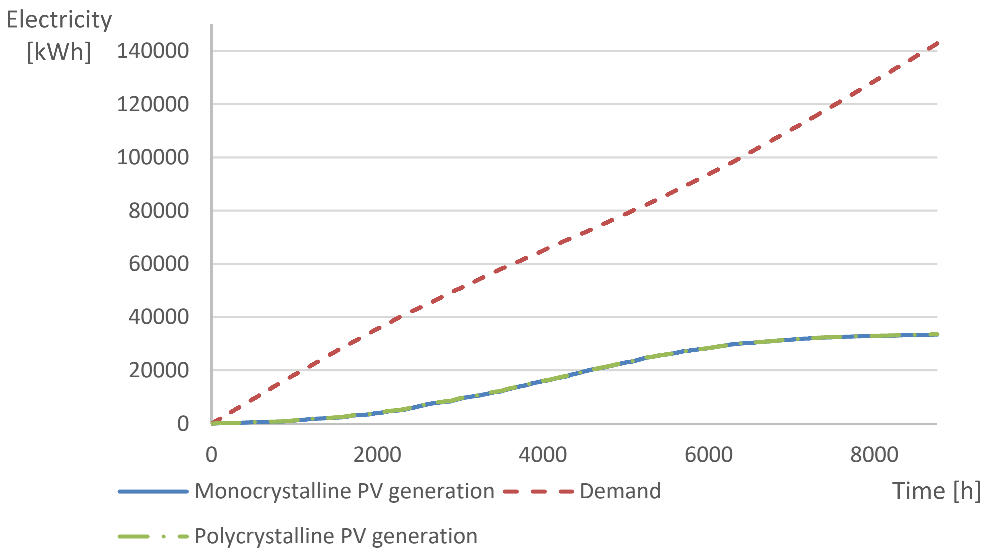

Figure 26. Cumulative electricity demand, monocrystalline and polycrystalline PV generation of the apartment block (occupants point of view)

Table 12. Monocrystalline PV system sizing results for the apartment block (energy company point of view)

Material	**Monocrystalline**			
Location	Roof part A	Roof part G	Roof part B	Roof part D
Modules per string	17	10	10	10
Strings	10	12	29	30
Number of inverters	6	6	6	8
Annual energy supply [kWh]	55237	39669	70531	85096
Annual energy sold to the occupants [kWh]	74393			
Annual energy bought from the occupants [kWh]	181925			
Total module area [m^2]	284.4	200.8	485.2	502
Nameplate capacity [kWdc]	60	42.4	102.4	105.9
Inverter model	ABB PVI-10.0-I-OUTD-x-US 208V	SolarRiver 7000TL-US 277V	Sunpower-10000-277V	Sunpower-10000-277V

Table 13. Polycrystalline PV system sizing results for the apartment block (energy company point of view)

Material	**Polycrystalline**			
Location	Roof part A	Roof part G	Roof part B	Roof part D
Modules per string	10	10	10	10
Strings	18	12	30	31

Number of inverters	6	3	7	6
Annual energy supply [kWh]	44291	29636	54928	66045
Annual energy sold to the occupants [kWh]	78417			
Annual energy bought from the occupants [kWh]	130466			
Total module area [m^2]	292.3	194.9	487.2	503.4
Nameplate capacity [kWdc]	46.8	31.2	78	80.6
Inverter model	SunPower 7501F 277V	Fronius IG Plus V10.0 277V	Fronius Primo 8.2-1 208V	Fronius Primo 8.2-1 208V

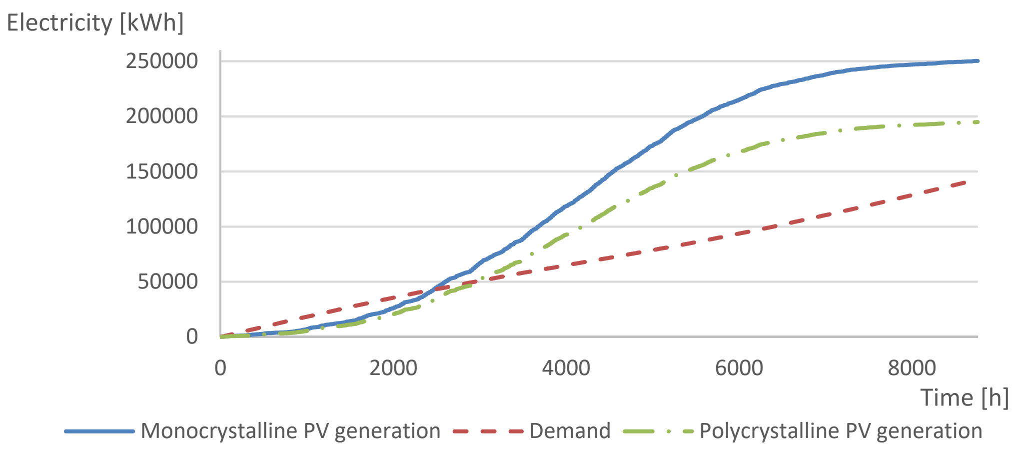

Figure 27. Cumulative electricity demand, monocrystalline and polycrystalline PV generation of the apartment block (energy company point of view)

4.3 Wind Energy

The weather file of Copenhagen is used to plot the wind direction and frequency, shown in Figure 28. The prevailing wind is from west and the wind velocity is approximately 35 km/h, and these will be used for wind velocity simulation in Autodesk Flow Design.

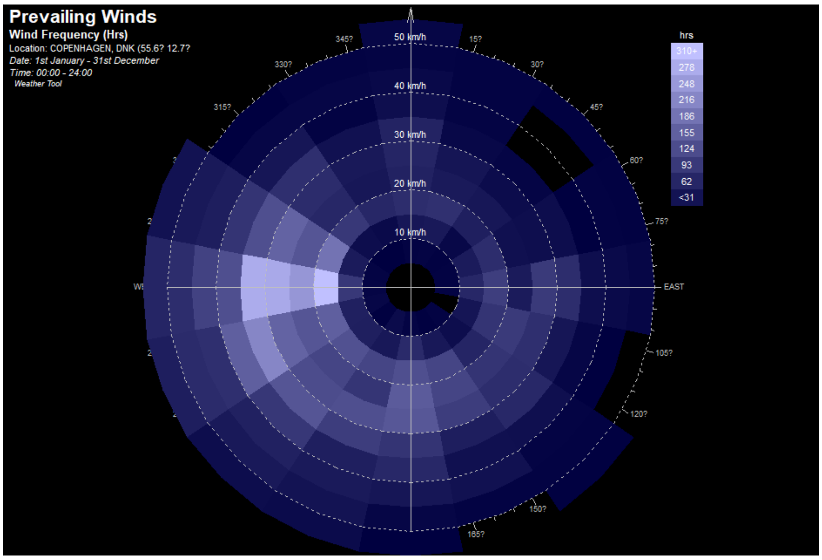

Figure 28. Wind Rose showing prevailing wind

As can be seen in Figure 29, the wind velocity is boosted by the parallel buildings along the street (tunnel effect). When the environment wind velocity is 10 m/s (annual average wind velocity), the wind velocity at selected spots can be higher than 8 m/s (see Figure 29). Figure 30 shows that the wind velocity at the rooftop level is as high as the environment, but the lower houses downstream are affected by the apartment buildings.

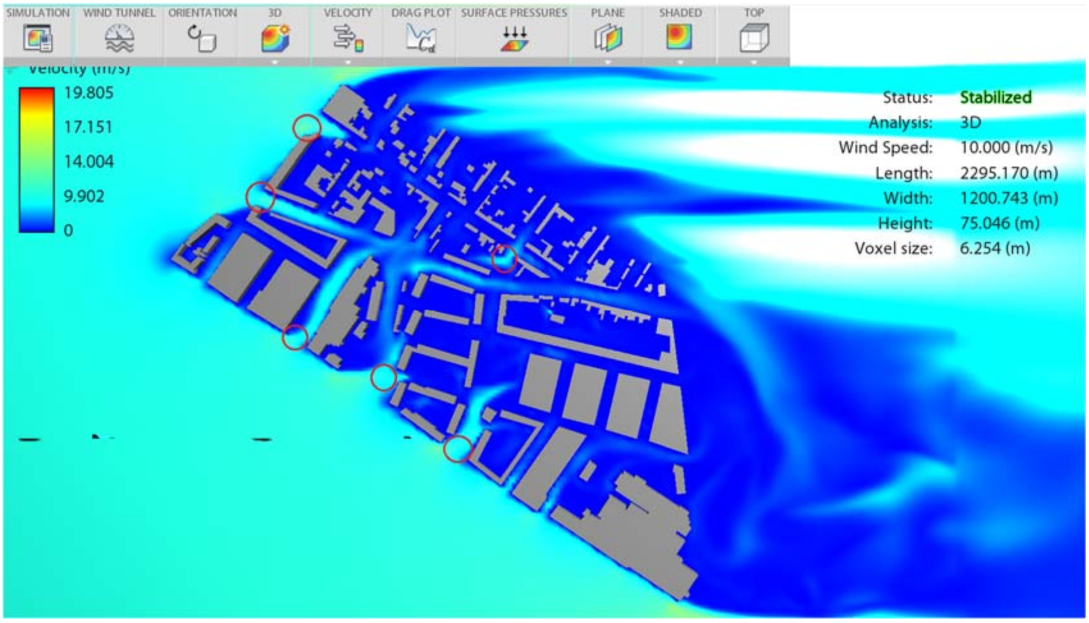

Figure 29. Wind velocity simulation in Sofielund neighborhood

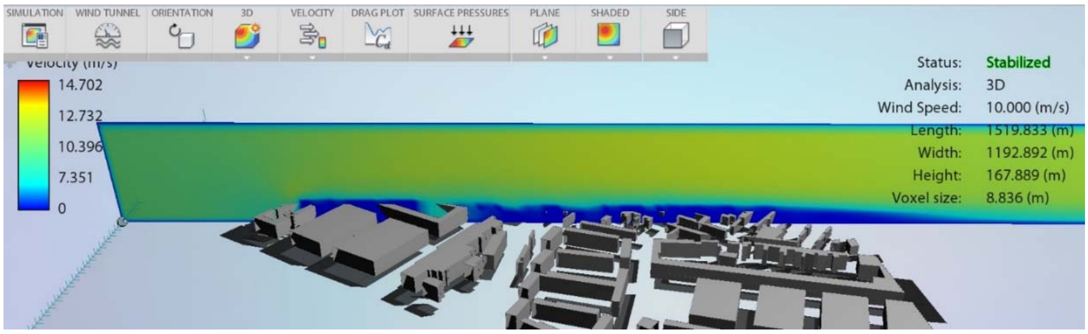

Figure 30. Wind velocity profile side view

VAWT is preferred in the built environment than HAWT and

shows the comparison between small VAWT models from Windside. Cut-in velocity of 2 m/s proves that once the wind velocity is higher than 2 m/s, the wind turbine starts to generate electricity, therefore a low cut-in velocity is important for turbines in urban environment. The annual average wind velocity for the selected spots in the neighborhood is 8 m/s and the estimated annual electricity output of WS12 is 22464 kWh, enough to supply electricity to around 1035 m^2 to 1182 m^2 of residential buildings. Figure 31 shows that if the annual average wind velocity increases from 8 m/s to 10 m/s, the annual electricity output will be doubled and the relationship between velocity and output is not linear, therefore the locations for wind turbines should be carefully selected. In addition, Windside micro wind turbines do not need to stop during the storms and the max power output is achieved during the storms. The noise level measured two meters away from the turbine is 0 dB, which is suitable to install in a residential neighborhood.

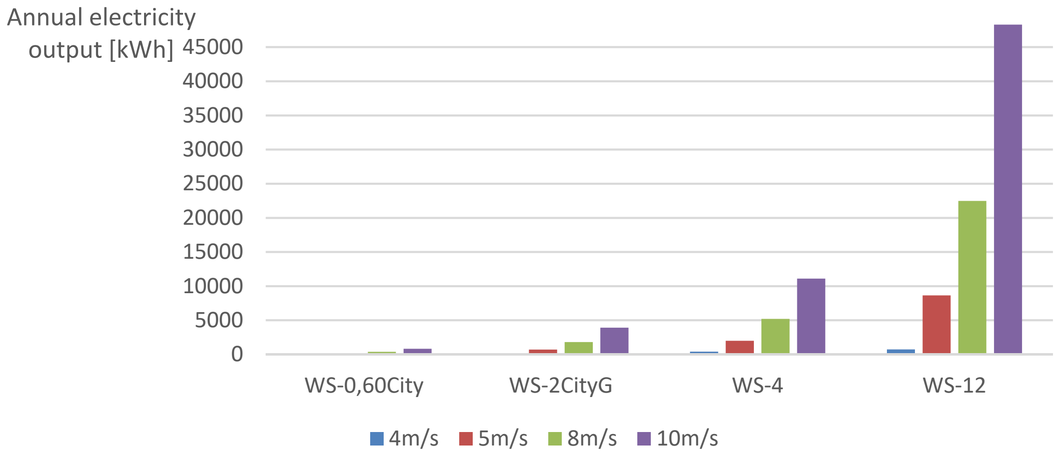

Figure 31. Estimated annual electricity output at annual average wind velocity

5 Discussion

In the studied residential neighborhood, there are mainly two types of buildings, single-family house and apartment block, the energy performance and renewable energy potential simulations on which are conducted. The heating and electricity demand of the entire neighborhood can be estimated by scaling with the living area or occupancy in the two sample buildings.

In this study, only one-year weather data from Energyplus is used to represent every year. However, considering the global warming and more and more frequent extreme weather, simulations on extremely warm year and extremely cold year should also be taken into consideration. When calibrating the thermal model settings, occupancy density, heating setpoint and infiltration rate are adjusted. These parameters have larger influence on the apartment block than the single-family house, due to the larger living area of the apartment block. There might be more settings affecting the heating demand, such as, heat recovery in the ventilation system and shading devices.

Several renewable energy sources are being utilized to replace the fossil fuel, including solar energy, wind, hydropower, tide power, geothermal and biomass, but some of these are limited by the location. In built environment, solar thermal collectors and PV panels are widely installed already, and in harbor cities, the annual average wind velocity is high, where the wind turbines are also possible to apply in the built environment. Ground source heat pump is applied in Western Harbor, where sea water and bed rock are the thermal storage. In order to utilize the geothermal energy in a sustainable way, the heat extracted from the ground during winter should be equal to the heat dissipated into the ground during summer. If only heat is extracted for heating, the ground temperature will gradually drop and the heat pump will not be as efficient.

Theoretically, in Sofielund neighborhood, there are houses and apartment buildings with large roof area, sufficient install PV panels. However, residents living opposite to the roofs can see the PV panels on the tilted roof, which can cause visual discomfort by reflecting the sunlight. As a result, the actual area to place panels is limited, not by the solar radiation, but by potential to cause visual discomfort, and then the Monocrystaline PV, which generates same amount of electricity but occupies the minimum space, is recommended. In addition, in order to install PV panels, a permission from Malmö city is required. It is also suggested that the energy company take part in the building design and construction process.

In terms of wind energy, only the annual electricity supply can be read from the table provided, and the hourly production is not available. In order for the corporation of solar panels and wind turbine, the hourly electricity output of the turbine should be determined. When the annual average wind velocity increases from 8 m/s to 10 m/s, the annual electricity output is doubled. This limits the applicability of built environment wind turbines to the cities with high average wind velocity.

6 Conclusion

The specific energy uses of the single-family house and the apartment block have exceeded the required value for non-electric heated buildings newly built in Sweden, by 21% and 60% respectively. The poor thermal performance can be predicted with the high U-values of the construction materials, as the buildings were designed and constructed in 1940s. After the energy retrofitting to the buildings, the design of the solar power installations will be different. Installing smart control to the building services system can also be considered to improve the energy efficiency in buildings. Applying time of use tariff is another way to achieve demand side control by stimulating the occupancy behavior, while trying to make full use of the renewable energy sources.

After the assessing the solar and wind power potential, it is appropriate to install the solar thermal, PV panels and micro wind turbine in the residential neighborhood in South Sweden. The solar thermal collectors are designed for the occupants DHW use only and does not go to the energy grid. The system can cover more than 50% of the annual DHW use, without boiling during summer and the space heating is still supplied with district heating. When sizing the PV system, there are two stands, the occupants and the energy company. The performances of monocrystalline PVs and polycrystalline PVs are similar when designed to cover the minimum hourly demand and avoid overproduction. However, monocrystalline generates more electricity than polycrystalline, if the whole roof is covered. For roofs facing East and West, the inverter size can be smaller, since the PV panels can never reach its maximum capacity. Since the electricity flow between generator, consumer and the grid takes place instantly, the buildings cannot be completely powered by PV system, if there is no battery. A smart grid with advanced control dispatching the energy flow between the generator, consumer and the grid should be developed. The wind velocity near the ground is low, because the rough surface slows down the wind. In order for the micro wind turbine to work well in the built environment, they should be installed to harvest the kinetic energy of wind at 15m level.

7 Summary

The modern technology has significantly changed people's lifestyle and energy demand. However, the energy crisis and energy source scarcity are the global issues to be solved. The built environment has contributed to approximately 40% of the global energy use. Therefore, countries in different part of the world are all introducing policies regarding the energy and environment issues. In European Union member states, all the buildings built by 2020 are required to be near zero energy. In terms of the utilization of renewable energy sources, Sweden is leading the world with 90% of the electricity supplied by nuclear power, hydropower and wind power plant. One of the largest cities in Sweden, Malmö, has the ambition to power the whole city with renewable energy sources by 2030.

The object studied is a single-family house and a residential block between the Malmö city center and suburb area, built in 1940s. The goal of the study is to evaluate the energy performance of the buildings in the neighborhood and assess the potential to apply renewable energy installations, including solar thermal, photovoltaic and wind power. The actual data of heating supply to the houses indicates that the houses lack automatic control over the heating terminals. Adding the thermostat to the heating system is beneficial to both the occupants' thermal comfort and energy performance.

The solar thermal collectors can cover 50% to 60% of the annual Domestic Hot Water demand, while the rest and space heating still require the district heating. If all the locations with sufficient solar radiation for PV installations are utilized, the monocrystalline system and polycrystalline system can generate 60% and 30% more electricity (than the actual demand) respectively. However, since the electricity flow between the consumer, PV system and the grid happens instantly, the buildings can never be off grid if there is no electricity storage equipment. This indicates the importance of smart grid and explains the sharp increase in the installed power of grid-connected PV system. The wind power conversion is not limited by the sunlight hours and can supply electricity during the high demand periods. However, the micro wind turbine energy generation is not simulated, so only the annual energy supply is available.

For further study, the wind turbines should be simulated to see the hourly energy supply. Geothermal energy should be utilized with a heat pump. Since there is no cooling for the residential buildings in Sweden, the cooling energy during summer should be delivered to the office buildings nearby to ensure the constant temperature of the ground. A Life Cycle Cost can be conducted to the renewable energy installations to check the economic feasibility. The Swedish policies regarding the renewable energy sources should be studied to check if the designs are valid in practice.

References

Alanne, K. and Saari, A. (2006). Distributed energy generation and sustainable development. Renewable and Sustainable Energy Reviews, 10(6), pp.539-558.

ASHRAE 62.1. (2010). Standards 62.1 & 62.2. [online] Available at: https://www.ashrae.org/technical-resources/bookstore/standards-62-1-62-2 [Accessed 18 Mar. 2018].

ASHRAE 90.1. (2013). Standard 90.1. [online] Available at: https://www.ashrae.org/technical-resources/bookstore/standard-90-1 [Accessed 18 Mar. 2018].

Autodesk.com. (2018). AutoCAD For Mac & Windows | CAD Software | Autodesk. [online] Available at: https://www.autodesk.com/products/autocad/overview [Accessed 13 May 2018].

Autodesk.com. (2018). Ecotect Analysis Free Download | Student Version for Academics. [online] Available at: https://www.autodesk.com/education/free-software/ecotect-analysis [Accessed 3 Mar. 2018].

Autodesk.com. (2018). Free Software for Students & Educators | Flow Design | Autodesk. [online] Available at: https://www.autodesk.com/education/free-software/flow-design [Accessed 13 May 2018].

Bahaj, A., Myers, L. and James, P. (2007). Urban energy generation: Influence of micro-wind turbine output on electricity consumption in buildings. Energy and Buildings, 39(2), pp.154-165.

Bernardo, R. (2017). Lecture in Photovoltaic Solar Cells. Helsingborg, Lund University.

Bernardo, L., Davidsson, H. and Andersson, E. (2016). Retrofitted Solar Domestic Hot Water Systems for Swedish Single-Family Houses—Evaluation of a Prototype and Life-Cycle Cost Analysis. Energies, 9(11), p.953.

Blair, N., Dobos, A. P., Freeman, J., Neises, T., Wagner, M., Ferguson, T., ... & Janzou, S. (2014). System advisor model, sam 2014.1. 14: General description (No. NREL/TP-6A20-61019). National Renewable Energy Laboratory (NREL), Golden, CO..

Cace, J., ter Horst, E., Syngellakis, K., Niel, M., Clement, P., Heppener, R. and Peirano, E. (2007). GUIDELINES FOR SMALL WIND TURBINES IN THE BUILT ENVIRONMENT. [online] Urban-wind.org. Available at: http://urban-wind.org/pdf/SMALL_WIND_TURBINES_GUIDE_final.pdf [Accessed 11 Mar. 2018].

Chen, Z., Guerrero, J. and Blaabjerg, F. (2009). A Review of the State of the Art of Power Electronics for Wind Turbines. IEEE Transactions on Power Electronics, 24(8), pp.1859-1875.

Dalenbäck, J. O. (1990). Central solar heating plants with seasonal storage: status report. Swedish Council for Building Research.

Dalenbäck, J. (2005). SOLAR HEATING – SWEDISH EXPERIENCE. [ebook] Available at: http://www.energiasostenible.org/mm/file/19_4-SolarThermalSystemsSweden.pdf [Accessed 25 Feb. 2018].

Davidsson, H. (2017). Lecture in Solar Collector Components. Helsingborg, Lund University.

Davidsson, H. (2017). Lecture in Solar Collector Technology. Helsingborg, Lund University.

Earthobservatory.nasa.gov. (n.d.). Climate and Earth's Energy Budget : Feature Articles. [online] Available at: https://earthobservatory.nasa.gov/Features/EnergyBalance/page3.php [Accessed 14 Mar. 2018].

Eliasson, I., Offerle, B., Grimmond, C. and Lindqvist, S. (2006). Wind fields and turbulence statistics in an urban street canyon. Atmospheric Environment, 40(1), pp.1-16.

Energytrust.org (2009). Calculating Inter-Row Spacing. [Online] Available at: http://energytrust.org/trade-ally/updates-and-events/InsiderNewsletter/insiderpdfs/100304_solarprofessional_article.pdf [Accessed 10 Mar. 2018].

Energy Informative (2015). Which Solar Panel Type is Best? Mono vs. Polycrystalline vs Thin film. [Online] Available at: http://energyinformative.org/best-solar-panel-monocrystalline-polycrystalline-thin-film/ [Accessed 26 Feb. 2018].

Faust, C. (2011). City of Sustainability and Renewable Energy. [online] Faustian urGe. Available at: https://spfaust.wordpress.com/2011/02/25/city-of-sustainability-and-renewable-energy/ [Accessed 10 Mar. 2018].

Grasshopper3d.com. (2018). Grasshopper. [online] Available at: http://www.grasshopper3d.com/ [Accessed 2 Mar. 2018].

Grasshopper3d.com. (2018). Ladybug Tools. [online] Available at: http://www.grasshopper3d.com/group/ladybug [Accessed 2 Mar. 2018].

Hang, Y., Qu, M., & Zhao, F. (2012). Economic and environmental life cycle analysis of solar hot water systems in the United States. Energy and Buildings, 45, 181-188.

Hanania, J., Stenhouse, K. and Donev, J. (2018). Betz limit - Energy Education. [online] Energyeducation.ca. Available at: http://energyeducation.ca/encyclopedia/Betz_limit [Accessed 12 Mar. 2018].

Hausner, R. and Fink, C. (2002). Stagnation behavior of solar thermal systems. [ebook] Gleisdorf. Available at: https://www.aee-intec.at/0uploads/dateien48.pdf [Accessed 15 Apr. 2018].

Iparraguirre, I., Huidobro, A., Fernández-García, A., Valenzuela, L., Horta, P., Sallaberry, F., Osório, T. and Sanz, A. (2016). Solar Thermal Collectors for Medium Temperature Applications: A Comprehensive Review and Updated Database. Energy Procedia, 91, pp.64-71.

Ishugah, T., Li, Y., Wang, R. and Kiplagat, J. (2014). Advances in wind energy resource exploitation in urban environment: A review. Renewable and Sustainable Energy Reviews, 37, pp.613-626.

Kalogirou, S. A. (2004). Solar thermal collectors and applications. Progress in energy and combustion science, 30(3), 231-295.

KARLSSON, R., & NILSENG, E. (2016). The potential for centralized photovoltaic systems in Sweden (Dissertation). Available at: http://urn.kb.se/resolve?urn=urn:nbn:se:kth:diva-189586

Li, T., Liu, Y., Wang, D., Shang, K. and Liu, J. (2015). Optimization Analysis on Storage Tank Volume in Solar Heating System. Procedia Engineering, 121, pp.1356-1364.

Lindahl, J. (2016). National Survey Report of PV Power Applications in Sweden. [ebook] International Energy Agency. Available at: https://www.energimyndigheten.se/globalassets/fornybart/solenergi/stod-till-solceller/national_survey_report_of_pv_power_applications_in_sweden_2014.pdf [Accessed 16 May 2018].

Malmo.se. (2016). 100% Locally Renewable Energy. [online] Available at: https://malmo.se/Nice-to-know-about-Malmo/Sustainable-Malmo-/Sustainable-Urban-Development/Western-Harbour/Energy.html [Accessed 15 Mar. 2018].

Malmo.se. (2008). Sustainable energy actions in four cities. [online] Available at: https://malmo.se/download/18.58f28d93121ca033d5e800086/1491299833011/secure_webb2.pdf [Accessed 15 Mar. 2018].

Manyeredzi, T. and Makaka, G. (2018). An Assessment of the Wind Power Generation Potential of Built Environment Wind Turbine (BEWT) Systems in Fort Beaufort, South Africa. Sustainability, 10(5), p.1346.

Matejicek, L. (2017). Assessment of Energy Sources Using GIS. Cham: Springer International Publishing.

Müller, G., Jentsch, M. and Stoddart, E. (2009). Vertical axis resistance type wind turbines for use in buildings. Renewable Energy, 34(5), pp.1407-1412.

Nilsson, P. (2007). World Clean Energy Awards: 100 % local, renewable energy in the Western harbour of Malm�, Sweden. [online] Cleanenergyawards.com. Available at: http://www.cleanenergyawards.com/top-navigation/nominees-projects/nominee-detail/project/59/?cHash=722e2f6bd2 [Accessed 15 May 2018].

Pickerel, K. (2015). What are the different types of solar modules?. [online] Solar Power World. Available at: https://www.solarpowerworldonline.com/2015/07/what-are-the-different-types-of-solar-modules/ [Accessed 20 Mar. 2018].

Resch, B., Sagl, G., Törnros, T., Bachmaier, A., Eggers, J., Herkel, S., Narmsara, S. and Gündra, H. (2014). GIS-Based Planning and Modeling for Renewable Energy: Challenges and Future Research Avenues. ISPRS International Journal of Geo-Information, 3(2), pp.662-692.

Saffari, M., de Gracia, A., Fernández, C., Belusko, M., Boer, D. and Cabeza, L. (2018). Optimized demand side management (DSM) of peak electricity demand by coupling low temperature thermal energy storage (TES) and solar PV. Applied Energy, 211, pp.604-616.

Solar Electricity Handbook. (2017). Solar Angle Calculator. [online] Available at: http://solarelectricityhandbook.com/solar-angle-calculator.html [Accessed 19 May 2018].

Svensksolenergi.se. (2015). Skandia Fastigheter, Väla Centrum. [online] Available at: https://www.svensksolenergi.se/om-oss/solenergipriset/skandia-fastigheter-vaela-centrum [Accessed 19 April 2018].

Rhino3d.com. (2018). Rhino Features. [online] Available at: https://www.rhino3d.com/6/features [Accessed 2 Mar. 2018].

Sam.nrel.gov. (2018). System Advisor Model (SAM) |. [online] Available at: https://sam.nrel.gov/ [Accessed 11 Mar. 2018].

Sommerfeldt, N., Muyingo, H., & af Klintberg, T. (2016). Photovoltaic Systems for Swedish Prosumers : A technical and economic analysis focused on cooperative multi-family housing. Stockholm. Retrieved from http://urn.kb.se/resolve?urn=urn:nbn:se:kth:diva-185003

Svekom (2003). City of Tomorrow. [ebook] Malmö. Available at: http://www.energie-cites.eu/db/malmo_566_en.pdf [Accessed 15 May 2018].

Pveducation.org. (2018). Hot Spot Heating | PVEducation. [online] Available at: http://www.pveducation.org/pvcdrom/modules/hot-spot-heating [Accessed 25 Feb. 2018].

PVEducation (2018). Module Circuit Design | PVEducation. [online] Pveducation.org. Available at: https://www.pveducation.org/pvcdrom/modules/module-circuit-design [Accessed 15 May 2018].

Urbangreenbluegrids.com. (2008). Bo01, Malmö, Sweden | Urban green-blue grids. [online] Available at: http://www.urbangreenbluegrids.com/projects/bo01-city-of-tomorrow-malmo-sweden/ [Accessed 15 May 2018].

Wang, C., Yang, X., Wu, Z., Che, Y., Guo, L., Zhang, S. and Liu, Y. (2016). A Highly Integrated and Reconfigurable Microgrid Testbed with Hybrid Distributed Energy Sources. IEEE Transactions on Smart Grid, 7(1), pp.451-459.

Weiss, W., Bergmann, I., & Stelzer, R. (2009). Solar Heat Worldwide, Markets and contribution to the energy supply 2007. IEA Solar Heating and Cooling Programme.

Windside.com. (2018). Windside - Products. [online] Available at: http://www.windside.com/products [Accessed 3 May 2018].

Winterscheid, C., Dalenbäck, J. and Holler, S. (2017). Integration of solar thermal systems in existing district heating systems. Energy, 137, pp.579-585.

Appendix A. Construction material layers

Table 14. Construction material of the external wall of the apartment block and the single-family house

Material	Thermal conductivity [W/(mK)]	Density [kg/m^3]	Specific heat capacity [J/(kgK)]	Thickness [mm]	U-value [W/(m^{2}K)]
Plaster board	0.17	800	1090	13	0.245
Mineral wool	0.04	80	840	145	
Air	0.25	10	1006	20	
Brick facade	0.9	1890	900	120	

Table 15. Construction material of the roof of the apartment block

Material	Thermal conductivity [W/(mK)]	Density [kg/m^3]	Specific heat capacity [J/(kgK)]	Thickness [mm]	U-value [W/(m^{2}K)]
Plaster board	0.17	800	1090	13	0.12
Mineral wool	0.04	80	840	245	
Fiber board	0.2	800	1090	3	
Air	0.25	10	1006	50	
Plaster board	0.17	800	1090	13	

Table 16. Construction material of the internal floor of the apartment block

Material	Thermal conductivity [W/(mK)]	Density [kg/m^3]	Specific heat capacity [J/(kgK)]	Thickness [mm]	U-value [W/(m^{2}K)]
Plaster board	0.17	800	1090	13	2.258
Concrete	0.7	1800	790	100	
Plaster board	0.17	800	1090	13	

Table 17. Construction material of the external floor of the apartment block

Material	Thermal conductivity [W/(mK)]	Density [kg/m^3]	Specific heat capacity [J/(kgK)]	Thickness [mm]	U-value [W/(m^{2}K)]
Water tight concrete	0.4	2800	960	300	1.016
Gravel	0.8	1800	790	50	

Table 18. Construction material of the internal wall of the apartment block

Material	Thermal conductivity [W/(mK)]	Density [kg/m^3]	Specific heat capacity [J/(kgK)]	Thickness [mm]	U-value [W/(m^{2}K)]
Plaster board	0.17	800	1090	13	-
Mineral wool	0.04	80	840	150	
Plaster board	0.17	800	1090	13	

Table 19. Construction material of the roof of the single family house

Material	Thermal conductivity [W/(mK)]	Density [kg/m^3]	Specific heat capacity [J/(kgK)]	Thickness [mm]	U-value [W/(m^{2}K)]
Plaster board	0.17	800	1090	13	1.015
Mineral wool	0.04	80	840	30	

Table 20. Construction material of the external floor of the single family house

Material	Thermal conductivity [W/(mK)]	Density [kg/m^3]	Specific heat capacity [J/(kgK)]	Thickness [mm]	U-value [W/(m^{2}K)]
Plaster board	0.17	800	1090	13	1.015
Mineral wool	0.04	80	840	30	

Table 21. Construction material of the external floor of the single family house

Material	Thermal conductivity [W/(mK)]	Density [kg/m^3]	Specific heat capacity [J/(kgK)]	Thickness [mm]	U-value [W/(m^{2}K)]
Plaster board	0.17	800	1090	10	2.422
Concrete	0.7	1800	790	100	
Plaster board	0.17	800	1090	10	

Table 22. Construction material of the internal wall of the single-family house

Material	Thermal conductivity [W/(mK)]	Density [kg/m^3]	Specific heat capacity [J/(kgK)]	Thickness [mm]	U-value [W/(m^{2}K)]
Plaster board	0.17	800	1090	10	-
Concrete	0.7	1800	790	100	
Plaster board	0.17	800	1090	10	

Appendix B. Occupancy Schedule

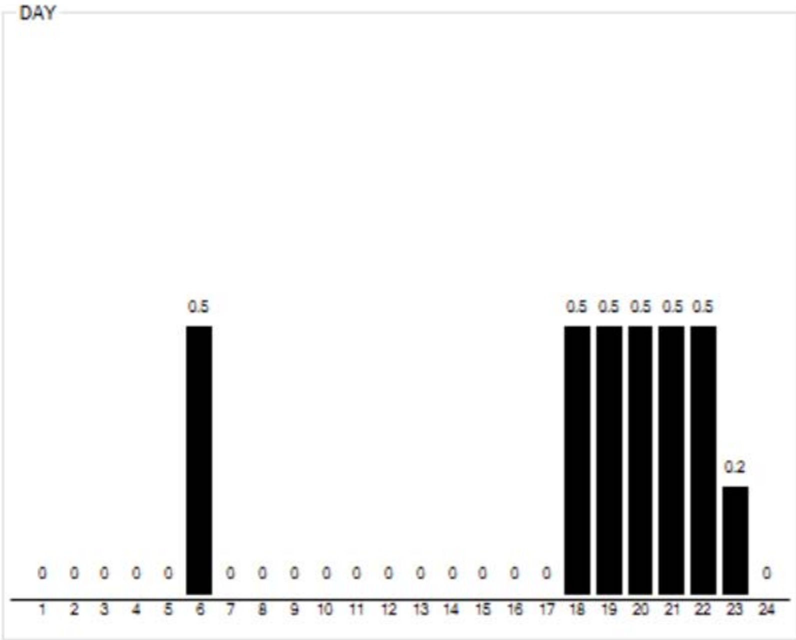

Figure 32. Day occupancy schedule of living room

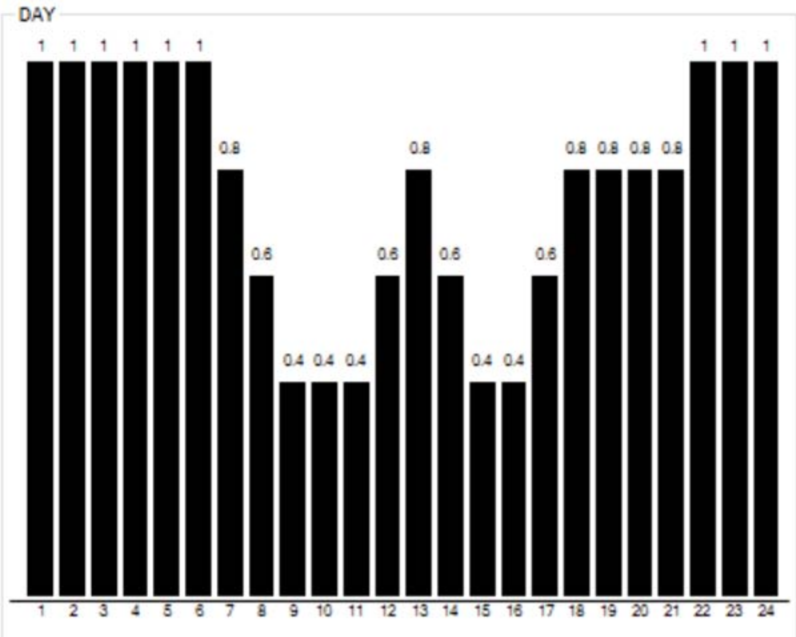

Figure 33. Day occupancy schedule of bedroom

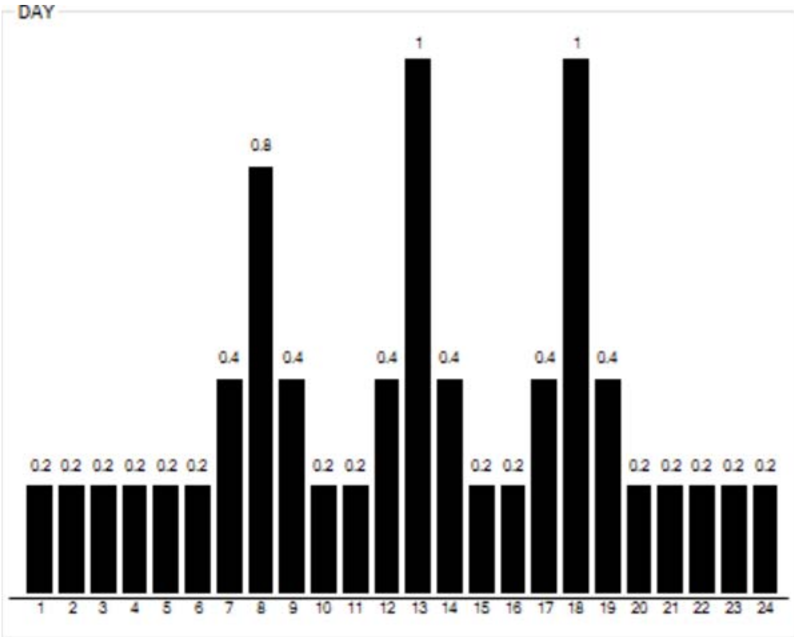

Figure 34. Day occupancy schedule of kitchen

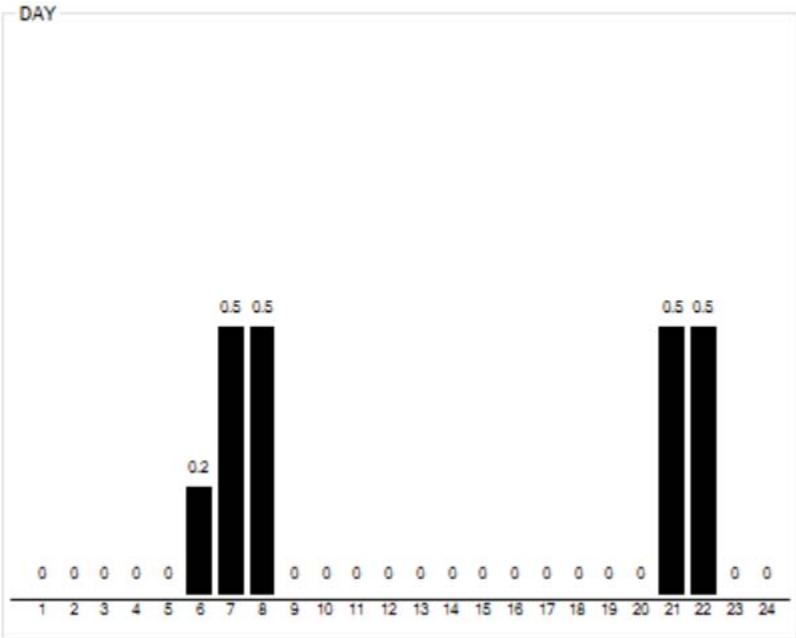

Figure 35. Day occupancy schedule of bathroom

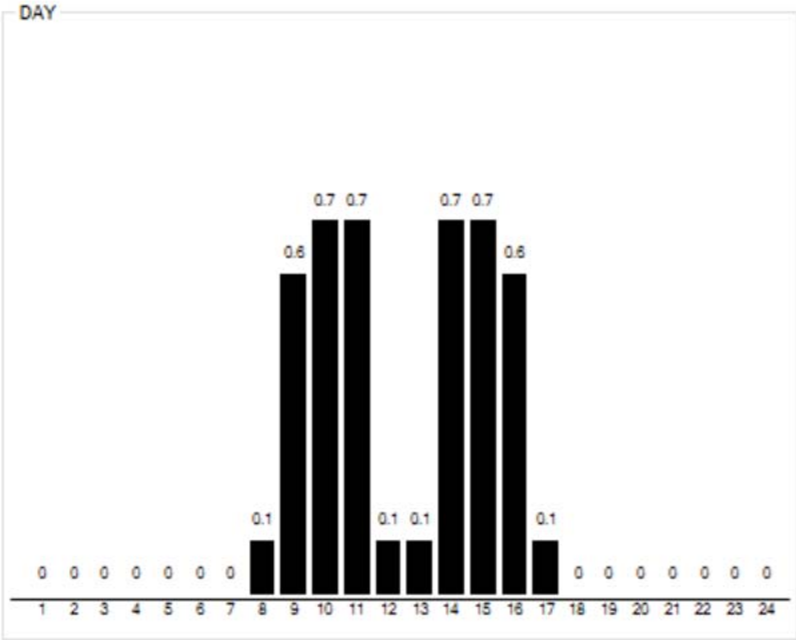

Figure 36. Day occupancy schedule of corridor

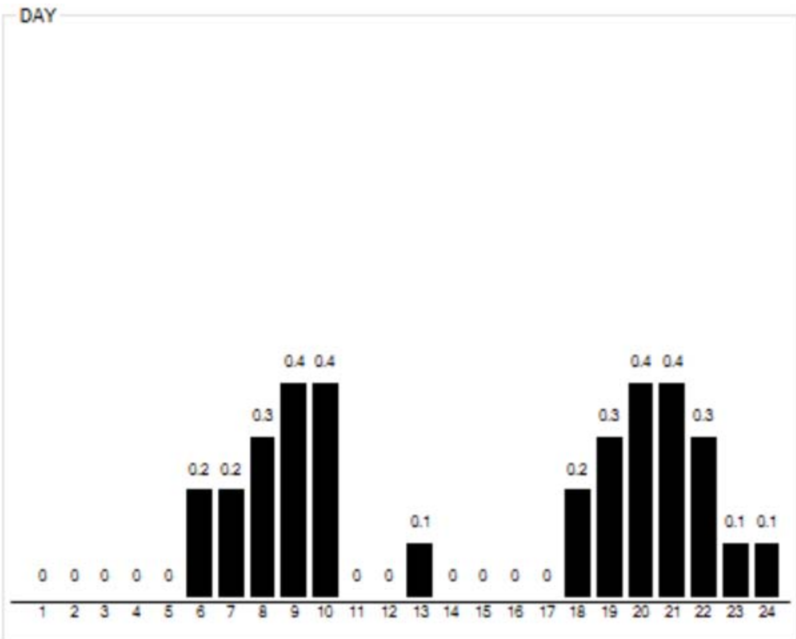

Figure 37. Day occupancy schedule of circulation

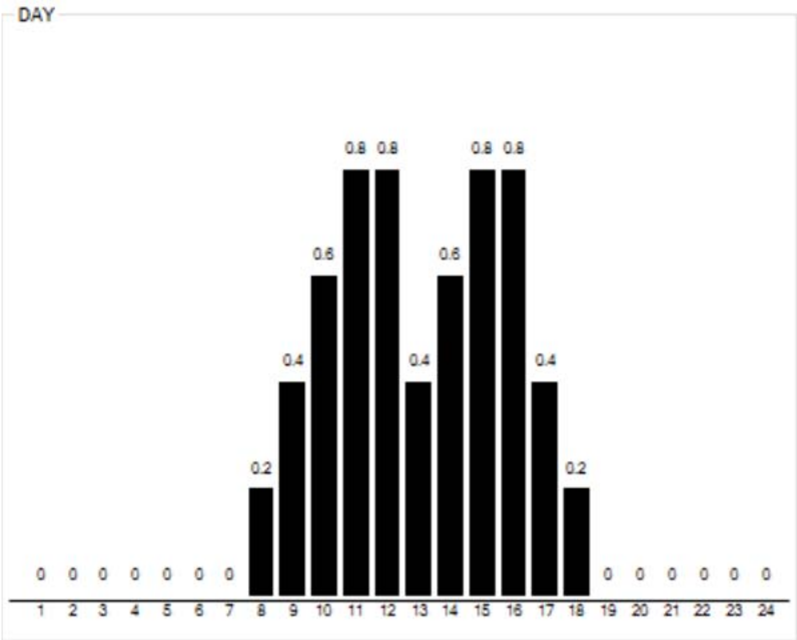

Figure 38. Day occupancy schedule of office

LUND UNIVERSITY

Dept of Architecture and Built Environment: Division of Energy and Building Design

Dept of Building and Environmental Technology: Divisions of Building Physics and Building Services